FACULTY OF BIOSCIENCE ENGINEERING

Functionality and *In-Vitro* Properties of Almond Gum-Shellac Nanoparticles Fortified with Quercetin

Vincent Kassozi

01600794

Promotor: Prof. Dr. Ir. Paul Van der Meeren

Tutor: Ali Sedaghat Doost

Master dissertation submitted in partial fulfillment of the requirement of the degree of International Master of Science in Nutrition and Rural Development: Human Nutrition

Academic Year 2017-2018

UNIVERSITEIT GENT

COPYRIGHT

……..

Prof. Dr. Ir. Paul Van der Meeren

Promoter

…….

Mr. Ali Sedaghat Doost

Tutor

……

Vincent Kassozi

Author

ACKNOWLEDGEMENT

Most importantly, I thank the **Almighty God** the author of everything in me; He indeed deserves all the praise and honor.

My promotor Prof. Dr. Ir. Paul Van der Meeren, thank you for the opportunity you gave me to work with and the tremendous support you have given me throughout. Mr. Ali Sedaghat Doost, you have been more than a tutor to me, you have provided me with the necessary knowledge and guidance. Thank you for being there for me all the time. I also extend my thanks to all the members of PaInT laboratory for their contribution towards my success. Dr. Ir. Charlotte Grootaert, thank for guidance and assistance.

I thank all the lecturers and instructors in all courses that I have attended for the two years, you have done a lot in shaping me into a credible person and of great relevancy. The ITC team, thank you for your support throughout the program.

Lastly, I want to thank VLIR-UOS scholarship for financially sponsoring my education and my entire stay in Belgium. I am so grateful for your contribution.

ABSTRACT

Quercetin (Q) is a flavonoid found in fruits, vegetables and some herbs. Q is known for its biological activity in the body, due to its beneficial impact on the risk of cardiovascular diseases, certain cancers, and inflammation. However, its application in food products is constrained by several factors including its low bioavailability, water solubility, bitter taste and chemical instability. Therefore, loading quercetin in nanoparticles (NPs) has been a vivid solution to overcome these challenges.

In this study, quercetin-fortified nanoparticles were prepared from shellac (SH) as the core material stabilized by almond gum (AG) and tween 80 (T80) using antisolvent precipitation method. The final nanoparticles were prepared by 0.67% SH, 0.02% Q, 0.5% AG and 0.1% w/v T80 using the stirring speed of 750 rpm at a dosing rate of 0.5 ml/min. The average particle size was 135±8nm with a polydispersity index (PDI) of 0.25±0.01, the encapsulation efficiency was 97.7±1.2%. The nanoparticles were also fully re-dispersible with a slight increase in particle size. Quercetin-loaded nanoparticles showed a high antioxidant activity at pH 7.4 compared to free quercetin while the degradation of quercetin was lower in the nanoparticles compared to free quercetin at the same pH. Although a high concentration of nanoparticles exhibited some toxicity towards Caco-2 cells, under subtoxic condition, cellular quercetin uptake was 3 times less than free quercetin. Quercetin loaded in nanoparticles was found to be 2 times more available for uptake than free quercetin at a pH of 7.4.

Key words: quercetin, nanoparticles, almond gum, shellac

TABLE OF CONTENTS

ACRONYMS

ABTS	2,2'-azino-bis(3-ethylbenzothiazoline-6-sulphonic acid
AG	Almond Gum
CVDs	Cardiovascular diseases
DMEM	Dulbecco's modified eagle medium
DMSO	Dimethyl sulfoxide
EE	Encapsulation efficiency
FRAP	Ferric reducing antioxidant power
FTIR	Fourier transform infrared spectroscopy
GSH	Glutathione
LC_{50}	Lethal concentration required to kill 50% of the population
MTT	3-(4,5-Dimethylthiazol-2-yl)-2,5 Diphenyltetrazolium Bromide
NCDs	Non-communicable diseases
NPs	Nanoparticles
PBS	Phosphate-buffered saline
PDI	Polydispersity index
Q	Quercetin
rpm	Revolutions per minute
SEM	Scanning electron microscopy
SH	Shellac
SRB	Sulforhodamine B
T80	Tween 80
TEM	Transmission electron microscopy
WHO	World Health Organisation

CHAPTER 1: INTRODUCTION

1.1 Background

Quercetin (*Figure 1*) is a naturally occurring flavanol found in fruits and vegetables such as apples and onions (Wu *et al*., 2008), herbs such as *Ginkgo biloba* (Watson & Oliveira, 1999) and red wine (Kerem *et al.,* 2004). In most plants, quercetin is bound to sugars, ethers and phenolic acids (Wang *et al.,* 2016). Quercetin in its pure form, exists as yellow crystals or powder with a bitter taste and poor solubility in water (0.01mg/ml at 25^{o}C) (Gao *et al*., 2011; Wang *et al*., 2016). It is however lipophilic and moderately soluble in ethanol (4mg/ml at 37^{o}C) (Priprem *et al*., 2008). Chemically, quercetin displays a typical flavonoid structure with five hydroxyl groups, two benzene rings (A and B) which are linked by an oxygen containing pyrene ring (C) (Wang *et al*., 2016).

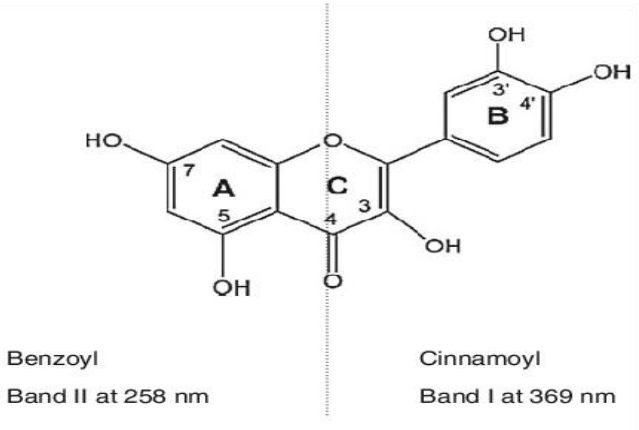

Figure 1: Chemical structure of quercetin

Quercetin and its biological activity have been extensively studied. Many studies have demonstrated that quercetin is a very strong antioxidant. It can scavenge reactive oxygen and nitrogen species and has the ability to chelate metal ions thereby preventing lipid peroxidation in the body (Bose & Michniak-Kohn, 2013; Kim *et al*., 2013; Kukongviriyapan *et al.,* 2012; Luangaram *et al.,* 2007; Arts *et al.,* 2004). Due to its antioxidant activity, several studies have linked quercetin to have strong anticancer properties (Cossarizza *et al*., 2011; Dajas, 2012). Its regular consumption has been related to reduced rates of lung, stomach, pancreatic, breast cancer (Damianaki *et al*., 2000), prostate cancer (Vijayababu *et al*., 2005) and colon cancer (Kuo, 1996; Park *et al*., 2005). Several unique properties have been reported for quercetin such as strong anti-inflammatory effects (Ruma, Sunil, & Prakash, 2013) as well as reduction in the

risk of coronary artery disease (Wang *et al*., 2016) and antimicrobial properties (Dinesh Kumar, Verma, & Singh, 2016).

Given all the above benefits of quercetin, there are however many technological challenges that limit the application of quercetin in food products. First, quercetin has a low solubility in water (Gao *et al*., 2011) coupled with a bitter taste. It is chemically unstable to oxygen, alkaline pH, temperature, other antioxidants and metal ions (Wang *et al*., 2016). Studies have shown that quercetin has a low bioavailability of 1% in humans (De Paz *et al*., 2015). Dietary blood concentrations of quercetin range from 10^{-9} to 10^{-7} M (Biasutto *et al*., 2010), which is lower than the therapeutic antioxidant concentrations ranging from 10^{-6} to 10^{-5} M (Vargas & Burd, 2010). Therefore, to enhance the dispersibility in aqueous systems, avoid degradation and improve the quercetin bioavailability, effective delivery systems are needed.

Different delivery systems of quercetin have been extensively studied and are successful to avoid quercetin degradation, to improve the aqueous dispersibility and to increase the bioavailability of quercetin (Aditya *et al*., 2014). Nanoparticles are one of these delivery systems that are currently explored. Due to their small size, nanoparticles have been found to enhance the solubility, increase the dissolution rate and enhance the absorption and bioavailability of drugs (Bhatia, 2016; Wu *et al*., 2008). For instance, Bagad & Khan (2015) showed that nanoparticles maintained a sustained release of quercetin and its bioavailability was strongly increased 2.38-4.93 fold compared to pure quercetin. In another study, it was revealed that the release of quercetin was improved 74-fold compared to pure quercetin and the antioxidant activity of quercetin was higher in nanoparticles than in pure form (Wu *et al*., 2008). However, it should be noted that most of these nanoparticles were prepared using many synthetic compounds and therefore their application in food products may be limited. Therefore, there is a growing demand especially from the food industry for quercetin-loaded nanoparticles fabricated from naturally existing compounds. In this study, nanoparticles were prepared using shellac (SH) as a core material, almond gum (AG) and tween 80 (T80) as stabilizers.

Shellac is a natural resinous product purified from lac which is secreted by Lac insects (*Kerria lacca*), which are tree parasites in India, Myanmar, Thailand and South China (Brown, 1973). It is composed of both polar and non-polar components comprising of polyhydroxy polycarboxylic esters, anhydrides and lactones (Patel *et al*., 2013). Shellac is insoluble in acidic and neutral pH (Leick *et al*., 2011) and it is physiologically harmless and has been proven to

be non-toxic (Farag & Leopold, 2009). Almond gum is produced by swe*et al*mond trees (*Amygdalus communis* L). This species mainly grows in subtropical regions especially Middle East, South East Asia (Ladizinsky, 1999) and the Mediterranean region (Bouaziz *et al*., 2014). It is classified as an arabinogalactan polysaccharide and consists of a water-soluble and water-insoluble fraction (Rezaei *et al.*, 2016). In this study, the water-soluble fraction was used. Tween 80, also known as polysorbate 80, is a synthetic nonionic emulsifier and surfactant. It is a derivative of polyethoxylated sorbitan and oleic acid (Food Safety Commission, 2007). The use of T80 in fabrication of nanoparticles has been shown to improve the encapsulation efficiency of the bioactive compound together with a reduction in particle size (Doost *et al*., 2018). In this study, the stability and in-vitro functionality of quercetin-loaded nanoparticles were studied. To this end, special attention was given to the creation of a high degree of supersaturation, a uniform spatial concentration distribution in the solution, and a negligible growth of crystals.

1.2 Objectives

To determine the effect of preparation parameters on particle size and acid resistance

- Determine the effect of stirring speed and dosing rate on particle size
- Determine the effect of AG and T80 concentration on particle size
- Determine the most optimal combination of ingredients that is resistant to aggregation at pH 1.2

To characterize the fabricated quercetin-loaded nanoparticles

- Measure the particle size of the fabricated quercetin-loaded nanoparticles
- Determine the encapsulation efficiency of quercetin by fabricated nanoparticles
- Study the morphology of the fabricated quercetin-loaded nanoparticles

To study the *in-vitro* functionality of quercetin-loaded nanoparticles

- Study the redispersability of the fabricated quercetin-loaded nanoparticles
- Study the antioxidant activity of quercetin-loaded nanoparticles
- Quantify the cellular uptake of quercetin-loaded nanoparticles using Caco-2 cells

CHAPTER 2: LITERATURE REVIEW

2.1 Nanoparticles

Nanoparticles are characterized by a particle size of less than 1000 nm. Because of their small size, nanoparticles enhance the absorption and bioavailability of drugs (Wu *et al*., 2008). They have been extensively used in the delivery of drugs with water-insoluble compounds (Bala *et al.,* 2006; Dai *et al.,* 2004). Some of the advantages of nanoparticles are: decreased patient-to-patient variability, enhanced solubility, increased oral bioavailability due to the increase in surface area, increased rate of dissolution and less amount of dose required (Bhatia, 2016).

2.1.1 Preparation of nanoparticles

Several methods have been used to prepare nanoparticles. Some of these are; spontaneous emulsification or solvent diffusion method (Murakami *et al.,*1999), double emulsion and evaporation (Ubrich *et al.,* 2004; Vandervoort & Ludwig, 2002), coacervation or ionic gelation (Fessi, Puisieux, Devissaguet, Ammoury, & Benita, 1989), polymerization (Boudad *et al.,* 2001) and anti-solvent precipitation (Kakran *et al*., 2012).

2.1.2 Anti-solvent precipitation method

Anti-solvent precipitation is attained through the addition of a non-solvent into a solution to achieve supersaturation. This is the driving force to solute precipitation (Joye & McClements, 2013).

The theory of anti-solvent precipitation is described by Kakran, Sahoo, Li, *et al*. (2012). It involves three steps: first, the generation of supersaturation, followed by nucleation, and lastly crystal growth. The anti-solvent precipitation method is mainly used for poorly water-soluble compounds. In this method, the compound is first dissolved in a solvent and is then rapidly mixed with a solvent-miscible anti-solvent. This leads to lowering of the solubility of the compound in the solvent as compared to the original solution, which results into supersaturation. The initial supersaturation (S) is given by Equation 1.

$$S = \frac{C_0}{C_{eq}}$$

Equation 1

where C_0 is the initial concentration of the solution to be precipitated and C_{eq} is the equilibrium concentration in the solute-solvent-anti-solvent system.

Nucleation is achieved when the solute concentration exceeds the equilibrium saturation concentration (Joye & McClements, 2013). The time elapsed between the onset of supersaturation and the appearance of nuclei is known as the induction time (Lyczko *et al*., 2002). Nuclei growth is achieved mainly by condensation happening when the solute concentration goes above the critical supersaturation concentration. Condensation occurs when molecules are added to the particle surface. It stops when the solute concentration goes below the equilibrium saturation concentration (Matteucci *et al*., 2006). The condensation rate is reduced by coagulation due to a reduction in the total number and surface area of present particles (Joye & McClements, 2013).

2.1.3 Important parameters

During the production of nanoparticles, it is important to control the particle size distribution and the stability of the particles (Thorat & Dalvi, 2012). It is desirable to produce small particles with low polydispersity index with stability against growth and gravitational separation (Joye & McClements, 2013). Changing various process conditions can lead to the control of these properties.

2.1.3.1 Anti-solvent to solvent ratio

Many studies have demonstrated that increasing the anti-solvent volume leads to a decrease in particle size (Bakldyga, Podgórska, & Pohorecki, 1995; Kakran *et al*., 2012; Khan & Schneider, 2013; Zhang *et al*., 2009). There are two explanations for this; first, increased instantaneous supersaturation resulting from the rapid reduction in solvent concentration (Kakran *et al*., 2012; Zhao *et al*., 2007); the second explanation is reduced crystal growth at lower solute concentration (Zhao *et al*., 2007).

2.1.3.2 Addition of solute to anti-solvent

The addition speed and order have been shown to have a major impact on the properties of the particles due to the influence on the rate and the degree of supersaturation, hence a nucleation and particle growth (Joye & McClements, 2013). Increasing the flow rate leads to increase in jet velocity, Reynolds number and shear forces. This results into increased mixing per unit time leading to a reduction in particle size (Kakran *et al*., 2012). Langer *et al*. (2003) discovered

that the addition rate had a substantial effect on the polydispersity index but no effect on particle size. Park, Jeon, & Yeo, (2006) found that the particle size was larger when anti-solvent was added to solute/solvent system.

2.1.3.3 Mixing

Mixing is a very important parament in the formation of nanoparticles since it helps to generate supersaturation which leads to nucleation and growth (Thorat & Dalvi, 2012). Mixing takes place at three different levels which are macromixing, mesomixing and micromixing. Macromixing occurs at a crystallizer scale, mesomixing is also known as turbulent mixing and involves large-scale mass transfer of the solution (Yu, Shekunov, Baldyga, & York, 2001). Mesomixing is influenced by solvent flow rate, stirring speed and turbulent diffusibility (Barrett *et al*., 2011). Micromixing involves molecular diffusion and engulfment of various solvent regions (Bałdyga, Bourne, & Hearn, 1997; Barrett *et al*., 2011). Micromixing directly influences the distribution of supersaturation and enables particles formed earlier with regions of high supersaturation as opposed to meso and macromixing which have an indirect effect (Joye & McClements, 2013).

2.1.3.4 Concentration of bioactive compound

The bioactive compound concentration also affects the particle size attributed to two mechanisms (Kakran *et al*., 2012; Meer, Sawant, & Amin, 2011). Number one, due to the high concentration of solute, the degree of supersaturation is increased, leading to the formation of more and smaller nuclei. However, nuclei growth will be promoted simultaneously due to the increased frequency of collisions and reduced diffusion distance. Secondly, when the solute concentration is increased, the viscosity also increases, which hinders diffusion between the solvent and anti-solvent leading to non-uniform supersaturation, slower nucleation rates and hence larger particles.

2.1.3.5 Temperature

Temperature has an impact on the precipitation process in many ways. It affects the equilibrium saturation and supersaturation, diffusion rate, and the velocity of the system. This in turn will have an impact on nucleation rate, crystal growth, coagulation, and agglomeration (Kakran *et al*., 2012; Kim *et al*., 2012). Generally, increasing the temperature leads to larger particles which have a broader particle size distribution (Park *et al*., 2006; Zhang *et al*., 2009; Zhao *et*

al., 2007). When the temperature is increased, the solubility of the compound also increases, this reduces the degree of supersaturation leading to the nucleation rate and thereby less particles grow into larger particles (Park *et al*., 2006). In addition, high temperatures increase the diffusion and hence promote the growth of particles.

2.1.3.6 Effect of stabilizers

Surfactants increase the nucleation rate by decreasing the interfacial tension forming smaller particles. Some polymers also have this effect and offer stabilization by steric hindrance or electrostatic repulsion (Joye & McClements, 2013). The properties of polymers like rigidity, polarity, and hydrophobicity also play a role in determining the ability of polymers to inhibit particle growth (Dalvi & Dave, 2009). At higher levels of surfactant, there may be the promotion of particle growth when the critical flocculation is exceeded (Joye & McClements, 2013).

2.2 Almond gum

Almond gum is produced by swe*et al*mond trees (*Amygdalus communis* L). This species mainly grows in subtropical regions especially Middle East, South East Asia (Ladizinsky, 1999) and the Mediterranean region (Bouaziz *et al*., 2014). The gum is produced from the branches, leaves and stems due to mechanical injury followed by microbial growth or because of gummosis disease (Ladizinsky, 1999).

2.2.1 Chemical composition of almond gum

Almond gum as well as Arabic gum, are classified as arabinogalactan polysaccharides due to the high composition of arabinose and galactose sugars (Rezaei *et al*., 2016). The composition of almond gum has been found to vary a lot depending on the region in which it is cultivated and the season (Rezaei *et al*., 2016). Rezaei *et al.*, (2016) found out that almond gum is composed of two main fractions that are classified based on their solubility in water, namely the water-soluble fraction and the water-insoluble fraction. This is used as a basis for determining the quality of gum; the higher the soluble fraction, the higher the gum quality. From their study, Rezaei *et al*., (2016) found that the soluble fraction of almond gum was about 90%. The water-soluble fraction is mainly composed of total sugars (93%) with some protein (0.16%), fat (0.12%) and ash (0.92%). The water-insoluble fraction has less sugars (58%), with higher protein (0.93%), fat (0.64%) and ash content (1.4%) than the water-soluble fraction.

The sugar composition of almond gum mainly comprises galactose and arabinose with small proportions of xylose, rhamnose, glucose and mannose (Rezaei *et al*., 2016). The whole gum and soluble gum have a higher galactose arabinose composition than the insoluble gum. Water soluble fraction is composed of arabinose (52.1%), galactose (33.42%), rhamnose (0.43%), mannose (0.18%), glucose (0.15%) and xylose (4.8%) (Rezaei *et al.*, 2016)

2.2.2 Applications of Almond Gum

Almond gum in Syria is mixed with palm gum to make Syrian gum for use locally in the confectionary industry. Irregular Eastern India gum is available in India, which is formed by mixing almond gum with other gums such as Arabic, tragacanth and ghati (Nussinovitch, 2009).

Almond gum has good emulsification properties and it has been revealed that less almond gum is needed to achieve optimal emulsification in comparison to Arabic gum (Mahfoudhi *et al*., 2014). Almond gum has also been reported to elongate the shelf life of sweet cherries (Mahfoudhi & Hamdi, 2015b) and tomatoes (Mahfoudhi, 2013). It has been demonstrated that Almond gum has antimicrobial activity on beef under cold storage (Bouaziz, *et al*., 2014).

2.2.2.1 Use of almond gum in nanoparticles

Hussain & Jaisankar (2017) used almond gum in the synthesis of hydrogel silver nanoparticles. In this study, almond gum was used to synthesize a semi interpenetrating hydrogel (almond gum-poly-acrylamide). The formed hydrogel was used to entrap silver nanoparticles. After formation, the nanoparticles were characterized, and the analysis of the antimicrobial activity was studied. The formed hydrogel silver nanoparticles exhibited a high thermal stability, which was attributed to the presence of silver nanoparticles inside the gel network. The effect of almond gum on swelling was also investigated and it was found that increasing in gum concentration increases the swelling capacity of the hydrogel silver nanoparticles up to 0.2g of gum. This was attributed to an increase in the hydrophilic groups. A further increase in gum resulted into a decrease in swelling capacity. This was due to the increase in the viscosity of the medium which inhibited the mobility of the ions. On the antimicrobial activity, it is reported that hydrogel silver nanoparticles exhibited a greater antimicrobial activity than semi interpenetrating hydrogels without silver nanoparticles. The greater antimicrobial activity was attributed to the sustained release of silver nanoparticles from the hydrogel.

Mahfoudhi & Hamdi (2015a) studied the kinetics and the storage stability of β-carotene encapsulated with almond gum and Arabic gum by freeze drying. Almond gum was found to have a higher encapsulation efficiency, smaller particle diameter and lower cold-water solubility than Arabic gum. On the storage stability, it was figured out that the relative humidity had a big role to play as the rate of degradation of β-carotene increased with increase in relative humidity for almond gum and Arabic gum. The degradation of both was also found to follow first order kinetics.

Rezaei *et al.* (2016) used almond gum/PVA nanofibers as a delivery system for vanillin. In this study, the nanofibers were formed by electrospinning. It was concluded that vanillin incorporated in almond gum/PVA nanofibers had a higher thermal stability than free vanillin.

Selvasudha & Koumaravelou (2017) compared the multifunctional synergistic effect of chitosan, almond gum and guar gum on simvastatin loaded nanoparticulate delivery system. In this study, nanoparticles were prepared by solvent evaporation.

2.3 Tween 80

Tween 80, also known as polysorbate 80 is a synthetic nonionic emulsifier and surfactant. It is a derivative of polyethoxylated sorbitan and oleic acid. Some of the hydroxyl groups of sorbitol and anhydrous sorbitol are esterified with oleic acid which is followed by condensation of about 20 ethylene oxide molecules (Food Safety Commission, 2007).

2.3.1 Use of Tween 80 in nanoparticles

Jacobs, Kayser, & Muller, (2000), prepared nanosuspensions for delivery of a poorly water-soluble drug (terazepide) and Tween 80 was used as a stabilizer. They discovered that the higher the concentration of the surfactant, the more stable the nanosuspension. Bhalekar *et al*. (2009), prepared solid lipid nanoparticles for topical delivery using T80 as a surfactant. They reported that an increase in T80 concentration led to a reduction in particle size. Wilson *et al*. (2008), prepared poly (n-butylcyanoacrylate) nanoparticles coated with T80 for delivery into the brain for treatment of Alzheimer's disease. It was discovered that the drug coated with T80 had a significantly higher uptake than the free drug.

2.3.2 Toxicity of T80

The toxicity of T80 has been widely studied (Castro *et al*., 1995; Müller *et al*., 1997; Tsujino, Yamazaki *et al*., 1999). Arechabala *et al*. (1999), studied the cytotoxicity of various surfactants,

both ionic and non-ionic, including T80. They reported T80 to have the lowest toxicity of the surfactants studied. The LC_{50} of T80 determined by MTT assay was 210µg/l. Müller *et al.* (1997), studied the cytotoxicity of solid lipid nanoparticles as a function of lipid matrix and the surfactant using the MTT assay. They reported that surfactants, including T80, which bind on the nanoparticles reduced further the toxicity of the nanoparticles.

2.4 Shellac

Shellac (*Figure 2*) is a resinous product purified from lac which is secreted by Lac insects (*Kerria lacca*), which are tree parasites in India, Myanmar, Thailand and South China (Brown, 1973). Shellac consists of polar and non-polar components comprising of polyhydroxy polycarboxylic esters, anhydrides and lactones. Aleuritic and terpenic are the main acid components (Patel *et al*., 2013). Shellac is insoluble in acidic and neutral pH (Leick *et al*., 2011). Shellac is physiologically harmless and has been proven to be non-toxic (Farag & Leopold, 2009).

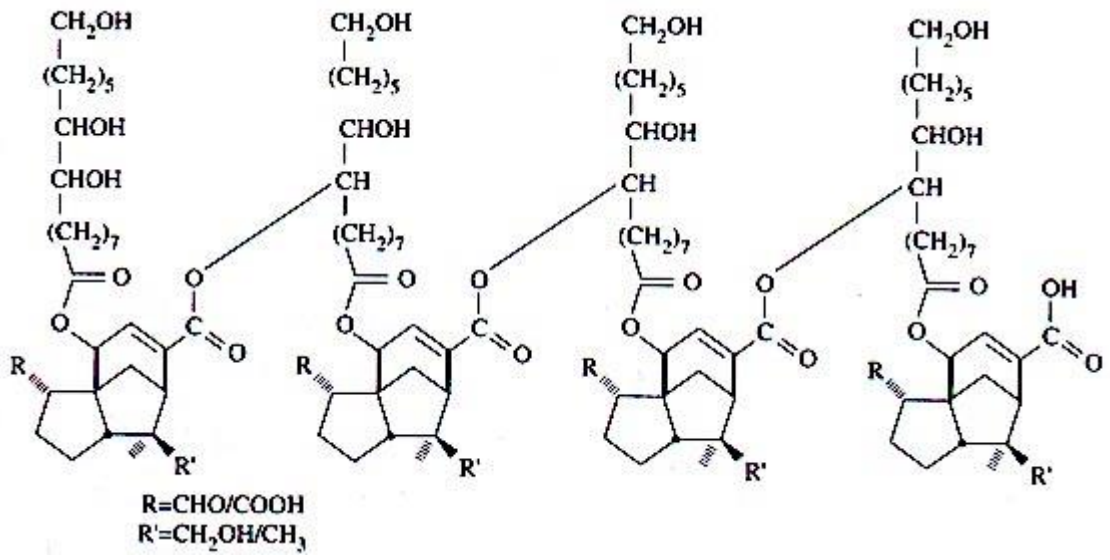

Figure 2: Chemical structure of shellac

2.4.1 Applications of shellac

Shellac is primarily used as an enteric coating due to its acidic character (Farag & Leopold, 2009). Shellac has been used for colon targeting. Roda *et al.*, (2007) developed a formulation with hydroxy methyl cellulose and shellac coating for extended and selective delivery of butyrate in ileo-caecal and colon. Wang *et al.* (2015) used shellac to form nanofibers for colon drug delivery. It has also been applied in the formulation of microcapsules (Sheorey *et al.*,

1991). Shellac has been used to prolong the shelf life of fruits such as oranges by acting as a coating material (Khorram *et al.*, 2017).

2.4.2 Use of Shellac in nanoparticles

Cui *et al.* (2014) prepared core-shell nanoparticles using shellac as the core material and polyvinyl pyrolidone as the shell material for drug encapsulation. The nanoparticles were prepared by electro-spraying. The used model drug was ferulic acid and the controlled release of this drug was studied. The formed nanoparticles had an average diameter of 530nm. From the drug release study, it was observed that the prepared nanoparticles could provide the desired drug release profile.

Characterization of the stability of curcumin zein-shellac nanoparticles was done by Sun *et al.* (2017). The nanoparticles were prepared by antisolvent co-precipitation. It was observed that the particle size was lower with bare nanoparticles compared to loaded nanoparticles. It is reported that the size of loaded zein-shellac was larger than that of loaded zein but smaller than that of loaded shellac. Zein-shellac nanoparticles showed a higher encapsulation efficiency than zein nanoparticles. Zein and shellac showed improved protection against the thermal degradation of curcumin. It was also noted that the zein-shellac complex allowed the controlled curcumin release in simulated gastrointestinal fluids.

In another study, shellac was used together with chitosan to form nanoparticles loaded with bovine serum albumin (BSA) (Kraisit *et al.*,2013). In this study, nanoparticles were prepared by ionic cross-linking. It was discovered that, depending on shellac, chitosan and BSA concentrations, three states could be observed that is; nanoparticles, aggregation and solution and this was due to electrostatic forces. A good balance between attraction and repulsion forces resulted into the formation of nanoparticles while aggregation and solution were formed due to an imbalance in these forces. The size of the nanoparticles ranged from 100 to 300nm. The encapsulation efficiency ranged from 11- 67%, while the loading efficiency ranged from 7-47% and the increase in chitosan glutamate resulted into a decrease in both due to the increase in viscosity. From the release study, it was observed that there was an immediate release of BSA and the release amount was between 64.3 and 78.1%.

Ma *et al.* (2017) prepared nanofibers and nanoparticles from shellac and sodium shellac for drug delivery. The drug loaded in these nanoparticles was ketoprofen. Nanoparticles were prepared by electro-spraying and electrospinning. The particle size diameter ranged from

351±250nm to 699±750nm depending on the components and the method of preparation. From the release study at pH 2, the release did not reach 100% due to agglomeration that was observed physically while at pH 6.8 100% release was achieved. It was also found out that sodium shellac had a larger drug release effect and a higher drug release rate than shellac. Likewise, nanoparticles had a larger drug release effect and higher drug release rate than nanofibers.

2.5 Quercetin

2.5.1 Chemical structure of quercetin

Figure 3 shows the chemical structure of quercetin (Wang *et al*., 2016); it exhibits a flavonoid structure with five hydroxyl groups. It has two benzene rings (A and B) with an oxygen containing pyrene ring (C) connecting both rings. The glycoside form of quercetin is the most common form in which quercetin is found. In this form, one or more hydroxyl groups are replaced by sugar groups of different types.

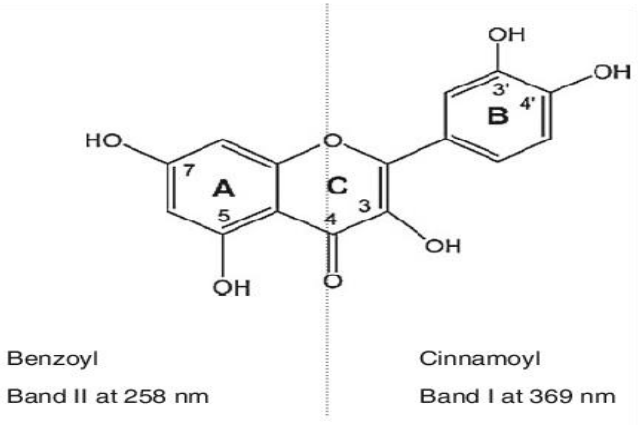

Figure 3: Chemical structure of quercetin

2.5.2 Biological activity of quercetin

The mechanism for antioxidant activity of Quercetin is based on its reactivity with reactive oxygen species and chelation of ions (Bose & Michniak-Kohn, 2013). Quercetin and other flavonoids are ideal scavengers of peroxyl radicals because of their favorable reduction potentials. The presence of a B-ring catechol group is responsible for scavenging reactive radical species through its hydrogen or electron donating ability (Schroeter *et al*., 2002). The presence of 2,3-unsaturation and 4-ortho group is partly responsible for the antioxidant activity

of quercetin. The ability to chelate redox-active metals is due to the presence of hydroxyl groups on the B-ring and the 5-hydroxy group of A-ring (Valko *et al*; 2006).

In vitro studies have revealed that quercetin is one of the most powerful scavengers of reactive oxygen species (Kim *et al*., 2013; Kukongviriyapan *et al.,* 2012; Luangaram *et al.,* 2007). These reactive species can induce damage of cells and tissues in the body which may result into cardiovascular diseases, cancer and diabetes (Valko *et al.,* 2006). Arts *et al.* (2004) presented that quercetin can enhance the endogenous antioxidant capacity of scavenging ABTS 6.2 fold compared to Trolox. Quercetin is reported to effectively protect cultured human skin fibroblasts, endothelial cells and keratinocytes against oxidative damage (Skaper *et al*., 1997). *In-vitro* and *in-vivo* studies have revealed that quercetin has strong anticancer properties (Cossarizza *et al*., 2011; Dajas, 2012). Quercetin prevents cancer induced by oxidative stress due to its antioxidant activity and the fact that it suppresses the activity of many kinases involved in the growth of cancer cells (Baghel *et al*., 2012). Quercetin has been reported to exhibit a strong anti-inflammatory capacity (Ruma *et al*., 2013). It is suggested that quercetin may suppress lipopolysaccharide-induced cytokine production in different cells (Wang *et al*., 2016). The anti-inflammatory activity of quercetin may be attributed to the antioxidative and free radical scavenging properties of quercetin (Comalada *et al*., 2005). The previous studies showed that quercetin can reduce the risk of coronary artery disease (Wang *et al*., 2016). Edwards *et al*. (2007) carried out a study on hypertensive patients; they found out that an intake of 730mg of quercetin per day reduced the systolic pressure by 7mm Hg, the diastolic pressure by 5mm Hg and the mean arterial pressure by 5mm Hg.

There are reports that diets high in quercetin may be vital in preventing blood clots and blocked arteries. This has been said to significantly reduce the chances of death from heart failure and stroke (Valko *et al*., 2006). Quercetin has also been described to have antimicrobial properties against food-borne pathogens. In study conducted by Dinesh Kumar, Verma, & Singh (2016), it was found that quercetin loaded nanoparticles were more effective against food-borne pathogens compared to free quercetin.

2.5.3 Chemical stability of quercetin

Quercetin has been shown to undergo chemical changes during food processing and storage The chemical stability of quercetin depends on oxygen concentration, pH, temperature, concentration of other antioxidants and metal ions (Wang *et al*., 2016).

Quercetin can undergo oxidation into different oxidation products which are referred to as quercetin-quinones (Boots *et al*., 2003). These products contain one ortho-quinone and three quinone methides. Quercetin can also undergo cleavage forming protocatechuic acid (Wang *et al*., 2016). The quercetin-quinones have been reported to be reactive towards mercaptans and can react with GSH instantly which is the most abundant endogenous mercaptan (Awad *et al*., 2002). At low GSH concentrations, quercetin-quinones can react with protein sulfhydryls to form protein-quercetin adducts known as glutathionyl-quercetin (Boots *et al*., 2003).

The stability of quercetin also depends on pH and temperature. Quercetin exhibits a high level of instability in organic solutions at pH >7 (Buchner *et al*., 2006; Young Moon *et al*., 2008). It has been revealed that the degradation of quercetin is higher under alkaline conditions (Buchner *et al*., 2006; Young Moon *et al*., 2008). Ranilla, Genovese, & Lajolo, (2009) reported a 70% quercetin loss in kidney beans when boiled at 100 ^{o}C for 50 min. They also reported that this loss is attained within 5 minutes under pressure cooking at 121^{o}C. Traditional pasteurization led to 17% decrease in quercetin in grapefruit juice (Igual *et al*., 2011).

Quercetin has also been reported to react with metal ions forming quercetin-metal complexes. This led to changes in redox potential of metal ions (Ravichandran, Rajendran, & Devapiriam, 2014). It is reported that this reaction leads to a reduction in the free radical scavenging activity of quercetin (Wang *et al*., 2016).

2.5.4 Bioavailability of quercetin

The food matrix has an important role in the bioavailability of quercetin (Wang *et al*., 2016). Goldberg, Yan & Soleas (2003) studied the absorption of quercetin in three different matrices (vegetable homogenate, grape juice, and white wine) in healthy individuals. Each contained 10mg quercetin/kg body weight and the subsequent serum quercetin concentrations were 10.8 ng/L for vegetable homogenate, 25.3 ng/L for grape juice and 12.7 ng/L for white wine.

2.5.5 Quercetin delivery systems

The available delivery systems for quercetin are currently divided into five groups: lipid-based carriers, polymer nanoparticles, inclusion complexes, micelles and conjugates-based nanoparticles (Wang *et al*., 2016).

Aditya *et al*., (2014) carried out a comparative study on three lipid nanocarriers for quercetin; solid lipid nanoparticles (SLN), nanostructured lipid carriers (NLC), and lipid nanoemulsions

(LNE). It was observed that quercetin loaded and free NLC had the smallest particle size compared to SLN (34nm) and LNE (47nm). The encapsulation efficiency in these systems was greater than 90%. LNE (58.4%) and NLC (52.7%) showed the highest bioaccessibility followed by SLN (39.7%) and lastly free quercetin solution (7%) at the end of two hours.

Bagad & Khan (2015), prepared quercetin loaded nanoparticles using poly (n-butylcyanoacrylate) (PBCA) coated with polysorbate-80 (T80) by emulsion polymerization method for oral delivery of quercetin. The particle size for quercetin-PBCA was 161.1nm and for quercetin-PBCA+T80 was 166.6nm. The encapsulation efficiency was found to be 79.86% for quercetin-PBCA and 74.58% for quercetin-PBCA+T80. There was an initial burst in the release. However, a sustained release was maintained compared to free quercetin. The bioavailability of quercetin was increased by 2.38-fold in quercetin-PBCA and 4.93-fold in quercetin-PBCA-T80.

Tan *et al*., (2011) prepared quercetin-loaded lecithin-chitosan nanoparticles using tocopheryl propylene glycol as a surfactant. The particle size was 95.3 nm and the encapsulation efficiency was 48.5%.

Wu *et al*. (2008) characterised the antioxidant activity of quercetin-loaded nanoparticles using eudragit and polyvinyl alcohol (PVA) as carriers by nanoprecipitation. The release of quercetin was increased 74-fold compared with pure quercetin. The antioxidant activity of the quercetin loaded nanoparticles was more effective than of pure quercetin on DPPH scavenging, anti-superoxide formation, superoxide anion scavenging, and anti-lipid peroxidation.

De Paz *et al*. (2015) produced water-soluble quercetin formulations by antisolvent precipitation and supercritical drying. It was observed that by using lecithin as a carrier material, it was possible to obtain stable and homogeneous dispersions of quercetin particles with high encapsulation efficiencies (up to 90%).

CHAPTER 3: MATERIALS AND METHODS

3.1 Materials

Quercetin (≥ 95%), Tween 80, dimethyl sulfoxide (DMSO, (≥ 99.5%)), and sodium azide (≥ 99.5%) were purchased from Sigma-Aldrich Co. Almond gum was bought from Sepahan Nano-Food Co. (Isfahan, Iran). The provided sample was white and of a uniform size without extra impurities and collected at a certain harvesting time from similar types of trees (*Amygdalus communis L.*). Shellac powder (SSB-55 PHARMA FP) with A particle size of 95% ≤100µm was kindly donated by SSB Stroever GmbH & Co. KG (Bremen, Germany). Ultrapure water purified by a Milli-Q filtration system (0.22µm) (Millipore Corp., Bedford, MA, USA) was used for the analyses and preparation of all aqueous solutions.

3.2 Extraction of almond gum

Almond gum was extracted using a procedure reported by Sedaghat Doost *et al*. (2018). Briefly, AG was pulverized with a ball mill (Retsch, PM 400, UK) for 30 minutes to create a powder. To separate the water-soluble fraction from the insoluble fraction, a stock solution (4%) in milli-Q water was left to stir for three hours at a temperature of 20^{o}C. For complete hydration, the mixture was kept at 4^{o}C overnight. The mixture was centrifuged at 20000rpm for 40 minutes at 25^{o}C and the clear solution (water-soluble fraction) was decanted off and 0.02% of sodium azide was added to prevent microbial growth. To determine the dry matter content, 10ml of the solution was dried at 105^{o}C overnight. The solution was kept at 4^{o}C for further experiments.

3.3 Preparation of nanoparticles

Nanoparticles were prepared by antisolvent precipitation. The procedure was adopted from Sedaghat Doost *et al*. (2018) with slight modifications. A Shellac stock solution of 2%w/v with (0.05%w/v) or without quercetin in ethanol (Absolute grade, VWR Belgium) was prepared and left to stir for 30 minutes. Absolute ethanol was used as the solvent while water was the antisolvent. The aqueous solution contained almond gum (0-0.7%w/v) and/or T80 (0-0.2%w/v). Nanoparticles were prepared by dosing of the ethanol solution in the aqueous solution using a dosing machine (Metrohm-765 Dosimat) at a set flow rate (0.1-9ml/min) while the aqueous solution was being stirred at a set stirring speed (500-1000rpm). The volumetric ratio of ethanol to aqueous phase was 1:3. The ethanol was evaporated off using a rotary

evaporator (IKA RV 10, Belgium) in a water bath at 50^{o}C at 190 mbar for 10 minutes. The final concentration of shellac was 0.67%w/v.

3.4 Effect of preparation parameters on particle size and acid resistance

3.4.1 Effect of stirring speed and dosing rate

In both studies, the nanoparticles were prepared with 0.67%w/v shellac and 0.5% almond gum. To determine the effect of stirring speed, the dosing rate was fixed at 6ml/min and the stirring speed was varied from 500rpm to 1000rpm. To study the effect of dosing rate, the stirring speed was kept constant at 750rpm while the dosing rate was varied from 0.1 to 9ml/min. The rest of the procedure remained the same as described in section 3.3.

3.4.2 Effect of almond gum and T80 concentration on particle size

Nanoparticles with different almond gum concentrations (0-0.7%w/v) were prepared with constant concentration of T80 (0.1%w/v). The dosing rate was 6ml/min while the stirring speed was 750rpm. The rest remained constant as described in section 3.3.

Nanoparticles with different T80 concentrations (0.01-0.2%w/v) were prepared with constant AG concentration (0.5%w/v). The dosing rate was 6ml/min while the stirring speed was 750rpm. The rest remained constant as described in section 3.3.

3.4.3 Acid resistance study

To determine the optimal combination of AG and T80 that prevents aggregation of shellac particles at pH 1.2 (stomach pH), the influence of pH on the visual appearance of 0.67%w/v shellac at different AG and T80 concentrations was investigated. The nanoparticles were diluted in milli-Q water and the pH adjusted to 1.2 with 1N HCl. The mixture was visually observed for aggregation.

3.5 Characterization of nanoparticles

The final nanoparticles were prepared using 2% SH (0.67% final composition), 0.05% Q (0.02% final composition), 0.5%w/v AG and 0.1%w/vT80. The stirring speed was 750rpm at a dosing rate of 0.5ml/min.

3.5.1 Size measurement

The particle size distribution of the samples was measured using Photon Correlation Spectroscopy (Model 4700, Malvern Instruments, U.K.) at a scattering angle of 150° at 25°C. The colloidal system was diluted prior to analysis with an appropriate solution (at pH 1.2 or Milli-Q water) to avoid multiple scattering. The light intensity correlation function was analyzed based on the CONTIN method, whereas the z-average diameter and PDI were obtained by cumulant analysis. Each individual measurement was an average of 10 runs.

3.5.2 Encapsulation efficiency (EE)

Quercetin encapsulation efficiency in the NPs was determined using UV spectrophotometry (UV-vis, VWR, Belgium) at 380nm. A standard curve (*Figure 4*) was generated using a series of quercetin concentrations ranging from 5-50µg/ml in DMSO (Sedaghat Doost *et al*,, 2018).

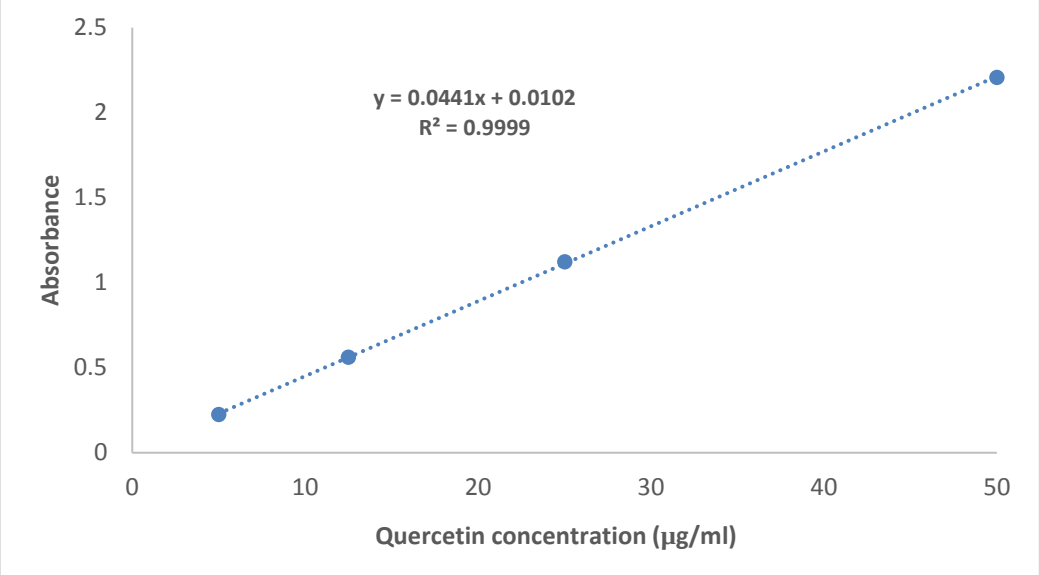

Figure 4: Standard curve of quercetin dissolved in DMSO

Encapsulation efficiency was determined based on the method reported by Davidov-Pardo *et al*., (2015). Briefly, a given amount of sample was placed in centrifugal tubes (Amicon altracel-10K 15ml, Millipore Cork Ireland). It was centrifuged at 3076g for 30min. The filtrate was dissolved in DMSO and the absorbance was read at 380nm. The concentration of quercetin was obtained from the standard curve. The EE was estimated as follows (**Equation *2***):

$$\text{EE } \% = \frac{CQ_1 - CQ_2}{CQ_1} \times 100$$

Equation 2

where CQ_1 is the concentration of quercetin added to the original sample and CQ_2 is the concentration of quercetin in the filtrate.

3.5.3 Morphology of nanoparticles

3.5.3.1 Cryo-Scanning electron microscopy (Cryo-SEM)

Cryo-SEM (JEOL Ltd, Tokyo, Japan) was employed to characterize the fabricated NPs. The selected sample was lyophilized using a freeze-drier (Alpha 1-2 LD plus, Christ) prior to SEM analyses. A small amount of sample was re-dispersed in Milli-Q water and placed on a copper grid. The sample was frozen in a nitrogen slush (-190°C) followed by fracturing. Then, it was sublimated for 30min and sputter coated with platinum prior to photograph recording.

3.5.3.2 Transmission electron microscopy (TEM)

The sample was diluted 1000 times with double distilled water and 2µl was blotted on a formvar-coated copper single slot grid (Agar Scientific). The copper grid was left to be dried under a fume hood at ambient temperature covered by a glass dish. The sample was visualized using a JEOl JEM 1010 (Jeol, Ltd, Tokyo, Japan) transmission electron microscope. Images were made with a Veleta side mounted CCD camera (EMSIS GmbH, Muenster, Germany).

3.5.4 Fourier transform infrared spectroscopy (FTIR)

Chemical structure changes of the freeze-dried quercetin loaded into shellac particles and pure quercetin were evaluated using Fourier transform infrared spectroscopy (Shimadzu IR Affinity-1, Kyoto, Japan). The FTIR spectra were recorded in a range of 4500-400 cm^{-1} wavenumbers and a 4 cm^{-1} resolution with 20 scans. The spectra were analyzed using LabSolutions IR software (V2.15, 2016).

3.6 Functionality and in-vitro properties of nanoparticles

3.6.1 Redispersability

The redispersability of the NPs was studied by dispersion of 10mg freeze-dried samples in 10ml Milli-Q water. The mixture was vortexed for two minutes and then left to be stirred at 30

rpm for one hour at ambient temperature (20°C). The particle diameter as well as PDI and visual appearance of the samples before and after freeze-drying were evaluated.

3.6.2 Antioxidant activity

The antioxidant activity of the released content of the NPs was carried out using the ferric reducing antioxidant power assay (FRAP). Firstly, the solutions of a) 20mM $FeCl_3.6H_2O$ in water, b) 10mM 2,4,6-tripyridyl-s-triazine in 40mM HCl, and c) 300mM acetate buffer with pH 3.6 were prepared. Secondly, a mixture of 2.5ml a and b with 25ml of C was incubated at 37°C for 5min prior to analysis. The sample with or without quercetin was first maintained at a pH of 1.2 and incubated at 37°C for 2h and then the pH was adjusted to 7.4 with 1N NaOH and incubated at 37°C for the next 2h. Finally, 30µl of the sample was mixed with 900µl of FRAP reagent, the mixture was kept for 4 minutes in an eppendorf and thereafter was centrifuged at 7000rpm for 3 min and supernatant transferred to a 1ml cuvette and the absorbance (at 593nm) was determined using a UV spectrophotometer (UV-vis, VWR, Belgium). A sample was analyzed at the beginning and then after every 30 minutes. Ascorbic acid solutions at different concentrations (67.5-500µM) were treated with the same method. The antioxidant activity value of the samples was calculated according to the method of Patel, *et al*. (2011)

3.6.3 Cellular quantification of quercetin levels using Caco-2 cells

3.6.3.1 Cytotoxicity tests

3.6.3.1.1 MTT assay

Caco-2 cells (ATCC) were grown under standard culture conditions (37°C, 10% CO_2) in high-glucose DMEM + glutamax (Fisher Scientific, Merelbeke, Belgium), supplemented with 1% non-essential amino acids (Fisher Scientific), 1% penicillin-streptomycin (Fisher Scientific) and 10% fetal bovine serum (FBS, VWR). For the toxicity test, cells were trypsinized, counted using Bürker counting chamber and Trypan blue staining (Sigma-Aldrich), and seeded in clear 96-well plates (Greiner) at a density of 20000 cells/well. After 24 hours of cell growth, the cells were incubated with either free quercetin, quercetin containing nanoparticles or quercetin-free nanoparticles, added to serum-free cell culture medium in different dilutions. After an overnight incubation, the cytotoxicity assays were started. For the MTT assay 100µL of cell culture medium was removed and 20µL of MTT (5 mg/mL stock in PBS, Sigma) was added. The mixture was then incubated in the dark at 37^o C and at 10% CO_2 for two hours. Thereafter,

the liquid was removed carefully and then 200µL DMSO was added and suspended. The absorbance was determined at 570nm using a Spectramax M2 Multimode Plate Reader (Molecular Devices, Berkshire, United Kingdom).

3.6.3.1.2 SRB assay

For the SRB assay, overnight treated cells were first fixed by addition of 50µL of 50% TCA (trichloroacetate in milli-Q water) and kept at 4^{o} C for one hour. The plates were rinsed with tap water and air-dried. Next, the cells were stained with 200 ml SRB solution (0.4% in 1% glacial acetic acid) for 30 minutes. The plates were then rinsed with 1% glacial acetic acid in milli-Q water, air-dried and the stain was resuspended in 200µL of 10mM Tris buffer. Thereafter, the absorbance was determined at 490nm using a Spectramax M2 Multimode Plate Reader.

3.6.3.2 Absorption of quercetin

The plate-reader method was initially proposed by Lee *et al*. (2014) and further optimized for the Caco-2 cell line by Vissenaekens (manuscript in preparation), and the fixation and staining methods were based on the papers from Grootaert *et al*. (2016) and Gonzales *et al*. (2016). Briefly, for the spectrofluorometric-based analysis, cells were trypsinized, counted using a Bürker counting chamber and Trypan blue staining (Sigma-Aldrich), and seeded in black 96-well plates (Greiner Bio One) at a density of 20000 cells/well. After the appropriate culture time, cells were exposed to the treatments in serum-free medium in a humidified incubator (37°C, 10% CO_2). After 24h of exposure, cells were gently washed with pre-warmed PBS (Sigma-Aldrich) and fixed with paraformaldehyde (4% in PBS) (Sigma-Aldrich) at 4 °C overnight. After this fixation step, cells were washed with ethanolamine (10mM in PBS) (Janssen Chimica, Beerse, Belgium) and PBS. Subsequently, cells were permeabilized with Triton-X100 buffer (0.5% in PBS) (Sigma-Aldrich) and washed with PBS. Then, cells were stained with diphenylboric acid 2-amino ethyl ester (DPBA) (0.2% w/v in 3% DMSO in water) (Sigma-Aldrich) for 2h at 37°C. For each condition, one replicate was loaded with 3% DMSO in water, without DPBA, to correct for background auto-fluorescence of the flavonoid. After 2h of staining, the cells were washed with PBS and finally 200 µL PBS was added to all samples to measure the DPBA fluorescence (λex/em=485/520 nm) using a Spectramax M2 Multimode Plate Reader. All data shown were corrected for background fluorescence.

3.7 Statistical analysis

The results are reported as mean ± standard deviation. A one-way analysis of variance was used to determine the differences in the results at 95% confidence interval. This was done after testing for homogeneity of variances with Levens test. Analyses were carried out by the R statistics package. MATLAB 2015 was used to estimate areas under the curves.

CHAPTER 4: RESULTS AND DISCUSSION

4.1 Effect of preparation parameters on particle size and acid resistance

4.1.1 Effect of stirring speed and dosing rate on particle size

Results showed an inverse relationship between stirring speed and particle size with 500rpm having the highest particle size and 1000rpm having the lowest particle diameter (*Figure 5*). On the other hand, there was no significant influence of stirring speed on PDI (data not shown). The reduction of particle size with increase in stirring speed is because rapid mixing ensures uniform and quicker distribution of the solvent leading to rapid supersaturation which induces quicker nucleation leading to smaller particles (Thorat & Dalvi, 2012). However, analysis showed no significant difference between 750rpm and 1000rpm, therefore, the mixing speed of 750rpm was selected as the most optimal since it consumes less energy and yet it can achieve the required particle size.

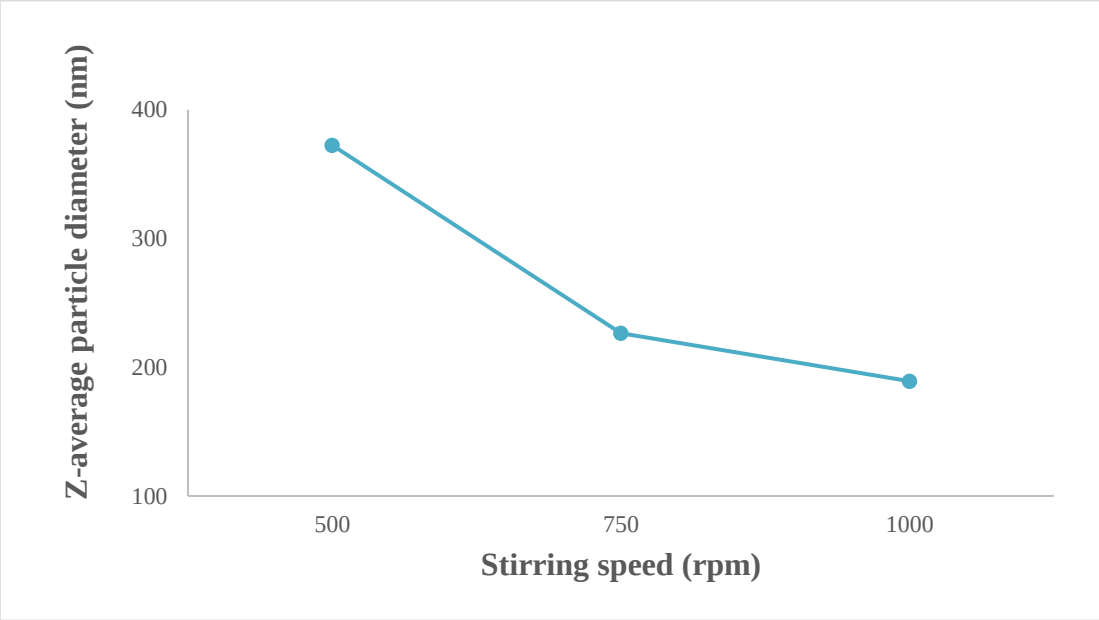

Figure 5: Effect of stirring speed on particle size – dosing rate (6 ml/min), 0.5%w/v AG and 0%w/vT80

The particle size was also observed to be affected by the dosing rate whereby an increase in dosing rate led to the formation of larger particles (*Figure 6*). For instance, the dosing rate of 9ml/min resulted into the largest particle size (395nm). Interestingly, there was no crucial impact of addition rate on polydispersity index. Our results were, however, in contradiction with Langer *et al*. (2003) who found an effect of dosing rate on polydispersity index but no

influence on particle size. The increase in particle size with dosing rate could be attributed to the effect of solvent to antisolvent ratio on particle size whereby the lower the ratio, the smaller the particle size and the higher the ratio, the larger the particle size (Bakldyga *et al*., 1995; Kakran, Sahoo, Tan, *et al*., 2012; Zhao *et al*., 2007). This implies that, at a lower dosing rate at any given point during dosing, the solvent to antisolvent ratio is lower. Hence, rapid nucleation occurred leading to smaller particles. However, when the dosing rate is increased, the solvent to antisolvent ratio is also increased leading to larger particles. In terms of particle size, 0.1ml/min gives the lowest particle size. However, in this study 0.5ml/min was selected for the subsequent experiments since 0.1ml/min is time consuming: it takes 40 minutes to add 4ml. This may make it difficult for application especially during upscaling on an industrial scale.

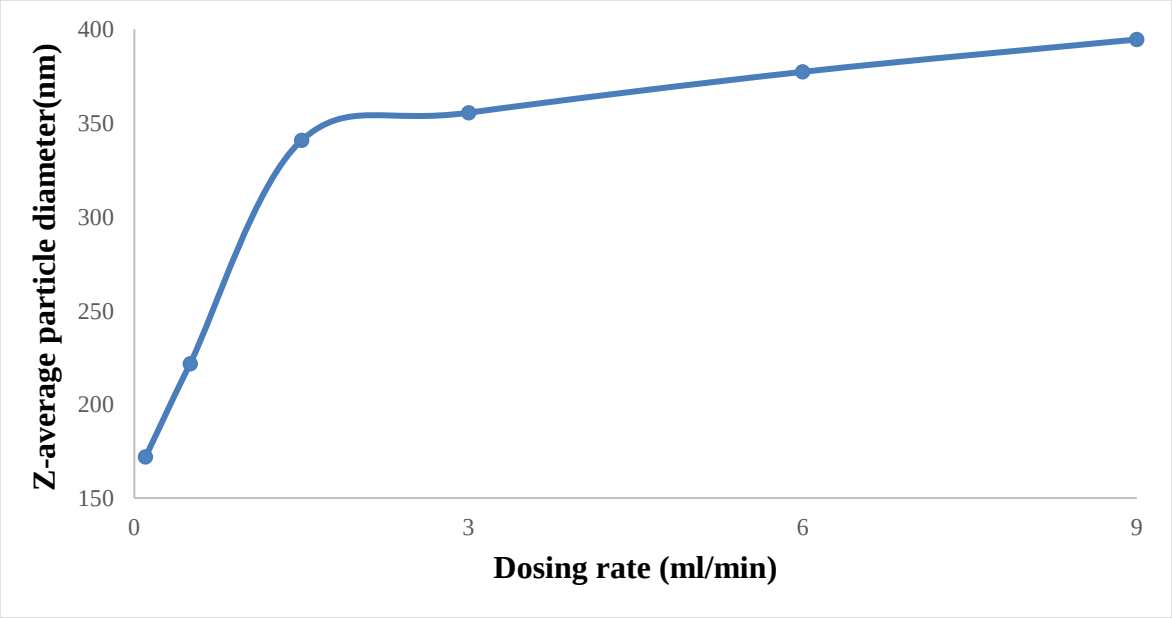

Figure 6: Effect of dosing rate of solvent to antisolvent on particle size – stirring speed (750rpm), 0.5%w/v AG and 0%w/vT80

4.1.2 Effect of almond gum and T80 (stabilizers) concentration on particle size

Generally, the results suggested a positive relationship between almond gum concentration and particle size (*Figure 7*) meaning that at higher AG concentration, larger particles were created. This can be explained by the increase in the viscosity which slows down the diffusion rate of solvent into the antisolvent delaying the nucleation rate, leading to fewer and larger particles (Meer *et al*., 2011). Thorat & Dalvi (2012) reported that an increase in polymer concentration enhanced flocculation leading to an increase in particle size.

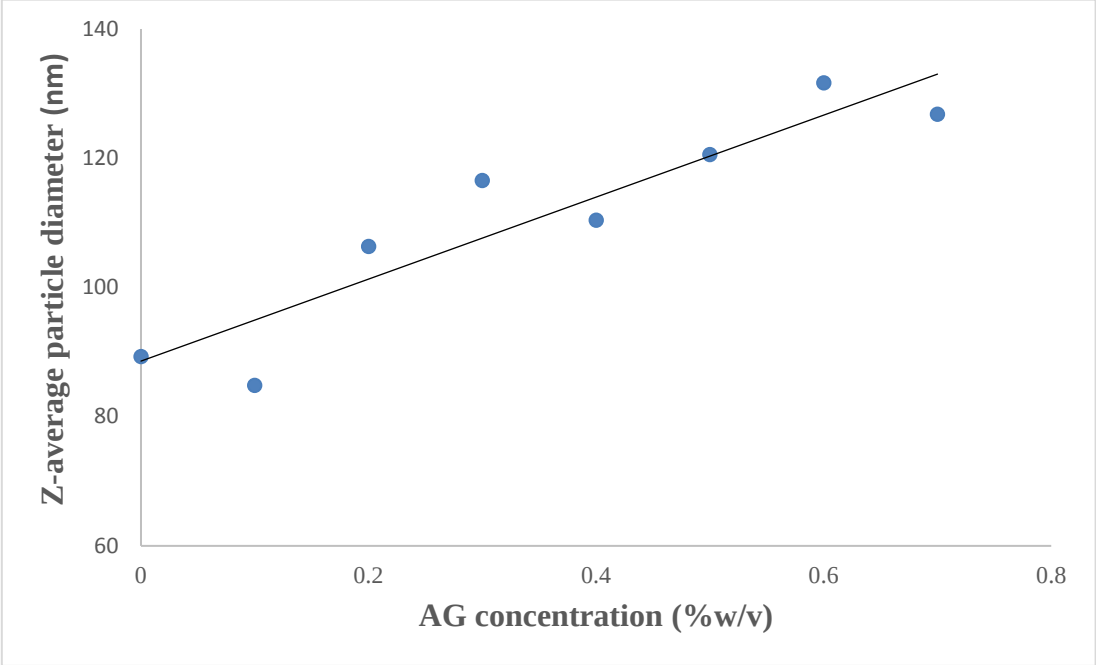

Figure 7: Effect of AG concentration on particle size at constant stirring speed (750rpm), dosing rate (6ml/min) and T80 concentration (0.1%)

From the results shown in *Figure 8*, it was evident that increase in surfactant (T80) concentration led to a decrease in particle size and polydispersity index. These results are in agreement with Sukmawati *et al*. (2018). However from 0.1 to 0.2% of T80, there was no significant further reduction in particle size and PDI (*Figure 8* and *Figure 9*). The decrease in particle size by increasing the T80 concentration could be due to the fact that T80 lowers the interfacial tension leading to rapid nucleation and hence formation of smaller particles (Joye & McClements, 2013). The lack of significant difference between 0.1% and 0.2%T80 is attributed to the fact that these two concentrations result in a similar effect on surface tension. The surface tension rapidly decreases with an increase in T80 concentration up to a given concentration, depending on the medium, and then it levels off (Pogorzelski *et al*., 2012). This implies that since there is no significant decrease in surface tension, there will therefore not be a significant effect on particle size and PDI.

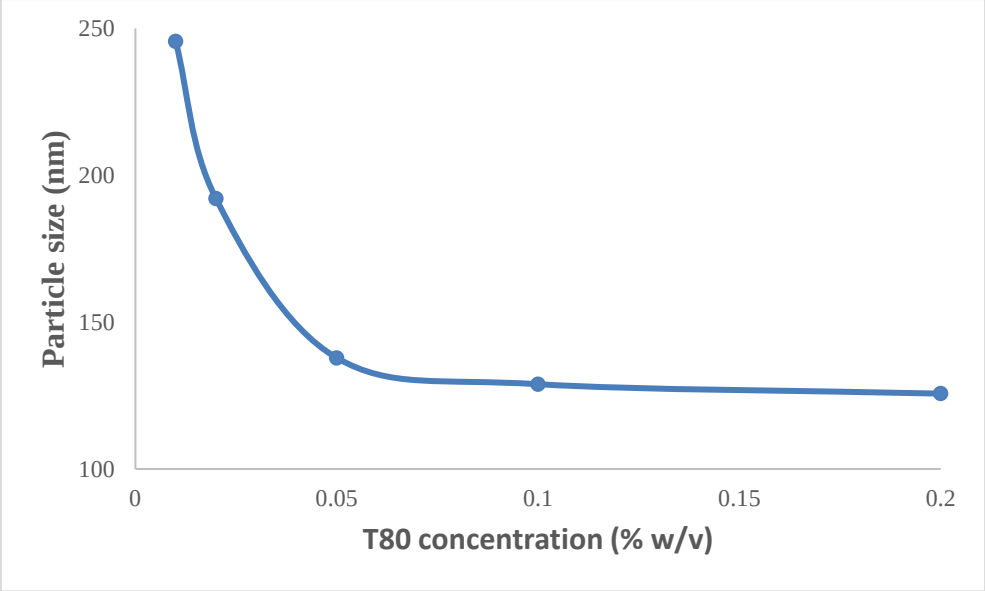

Figure 8: Effect of T80 concentration on particle size at constant stirring speed (750rpm), dosing rate (6ml/min) and AG concentration (0.5%)

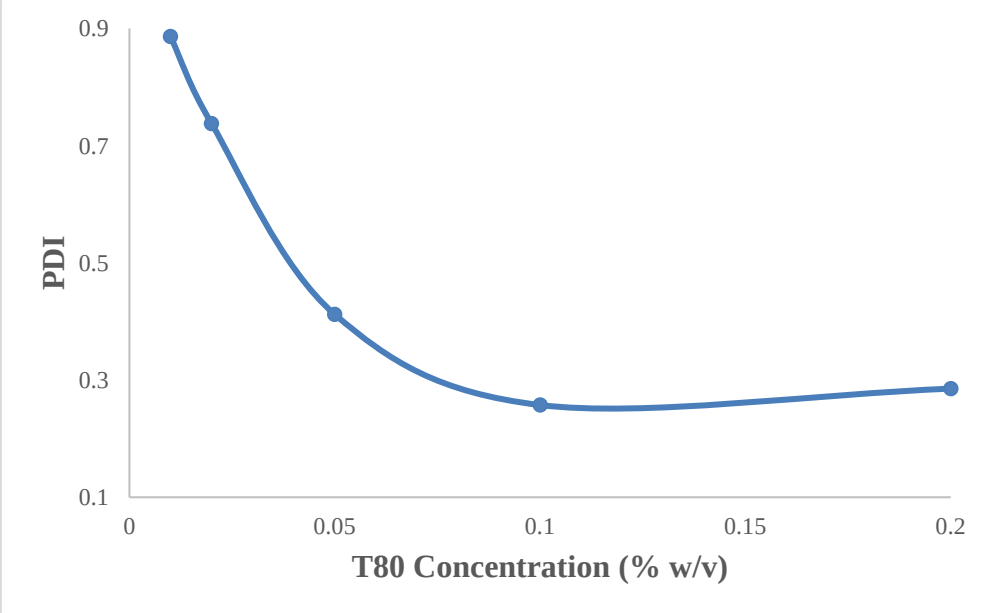

Figure 9: Effect of T80 concentration on PDI at constant stirring speed (750rpm), dosing rate (6ml/min) and AG concentration (0.5%)

4.1.3 Acid resistance study

The solubility of shellac in water is pH dependent, it is soluble at pH above 7 while below pH 7, it tends to be less soluble. Moreover, at very low pH such as a stomach pH (1.2), shellac precipitates (Patel *et al*, 2011). This precipitation of shellac is not desirable because it leads to large particles with significantly lower surface area to volume ratio. This leads to reduced

absorption and bioavailability of the bioactive compound. Therefore, the purpose of this study was to come up with the most optimal formulation that could ensure stability of shellac at stomach pH. From *Figure 10*, it was observed that shellac alone greatly aggregated while a combination of shellac and AG or shellac and T80 showed an improvement as can be seen from the turbidity of the samples. However, this was not sufficient to fully prevent precipitation. However, a combination of shellac with AG and T80 was found to be very resistant to aggregation which could be due to the protection that AG and T80 offer by coating the shellac nanoparticles and hence prevent them from precipitating. AG coats shellac nanoparticles, while T80 being a nonionic surfactant provides further coating and renders stability of the nanoparticles by steric repulsion (Asasutjarit *et al*., 2013). Patel *et al*. (2011), reported aggregation of simple shellac colloidal particles while when shellac was combined with xanthan gum, the resulting particles were stable at pH 1.2.

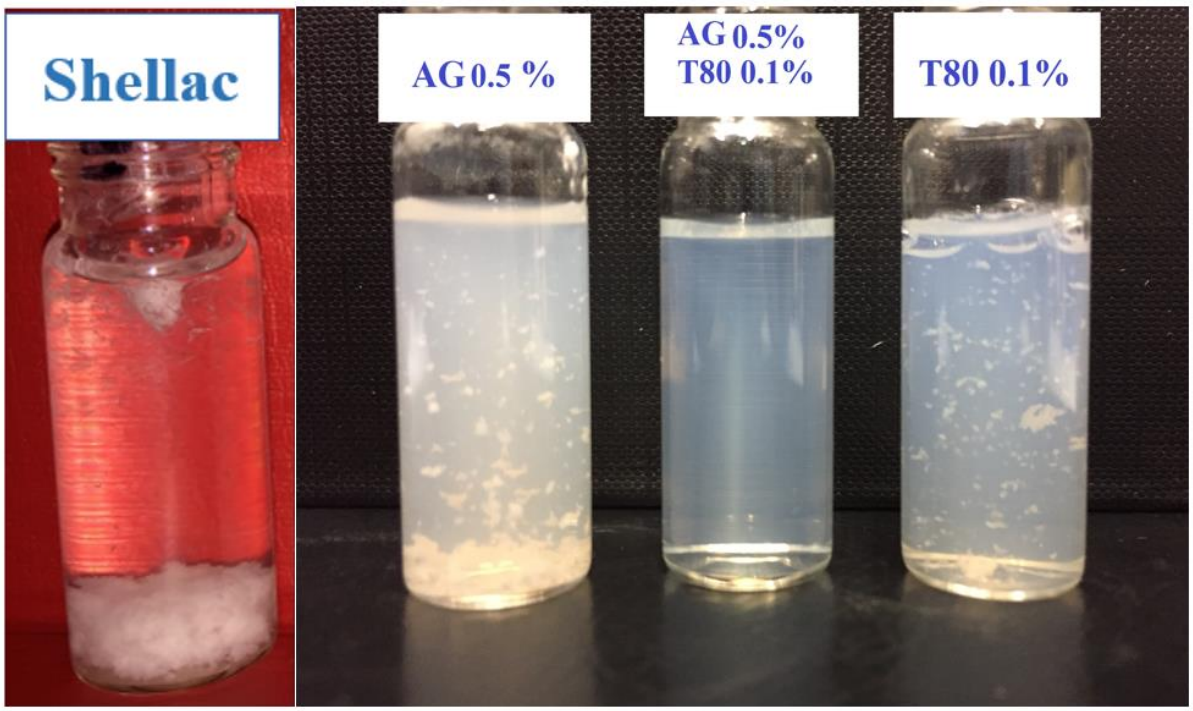

Figure 10: Stability of nanoparticles (not loaded with quercetin) under stomach conditions (pH 1.2)

4.2 Characterization of nanoparticles

4.2.1 Size measurement

Particle size is a very vital parameter in characterization of nanoparticles. It helps to determine the quality of the fabricated nanoparticles. Smaller particles are desirable because they have a

larger surface area to volume ratio which is very relevant in improving the absorption and bioavailability of the bioactive compound (Bhatia, 2016; Wu *et al*., 2008) and are considered to have more physicochemical stability (Joye & McClements, 2013). The fabricated nanoparticles had an average particle size of 135±8nm with a PDI of 0.252±0.01 and with a monomodal distribution (data not shown). Our results were in agreement with the work performed by Sedaghat Doost *et al*. (2018), but with a different preparation method.

4.2.2 Encapsulation efficiency

Encapsulation efficiency is an important parameter for measuring the amount of the bioactive compound entrapped within the nanoparticles. It is desirable for the encapsulation efficiency to be as close to 100% as possible. High encapsulation efficiency has been associated with better targeted delivery (Vashisth *et al*., 2015). In this study, the nanoparticles had an encapsulation efficiency of 97.7±1.2%. This result was comparable to the results obtained by Sedaghat Doost *et al*. (2018) who prepared the nanoparticles containing quercetin.

4.2.3 Morphology of nanoparticles

The Cryo-SEM photographs presented in *Figure 11*, confirm the morphology and size of the nanoparticles. As it can be seen, the particles are mostly spherical with rough surfaces. The roughness of the surfaces is due to the AG and T80 coating of the core material (SH and Q). The particle diameter was also close to 100nm consistent with the particle size obtained from the DLS technique.

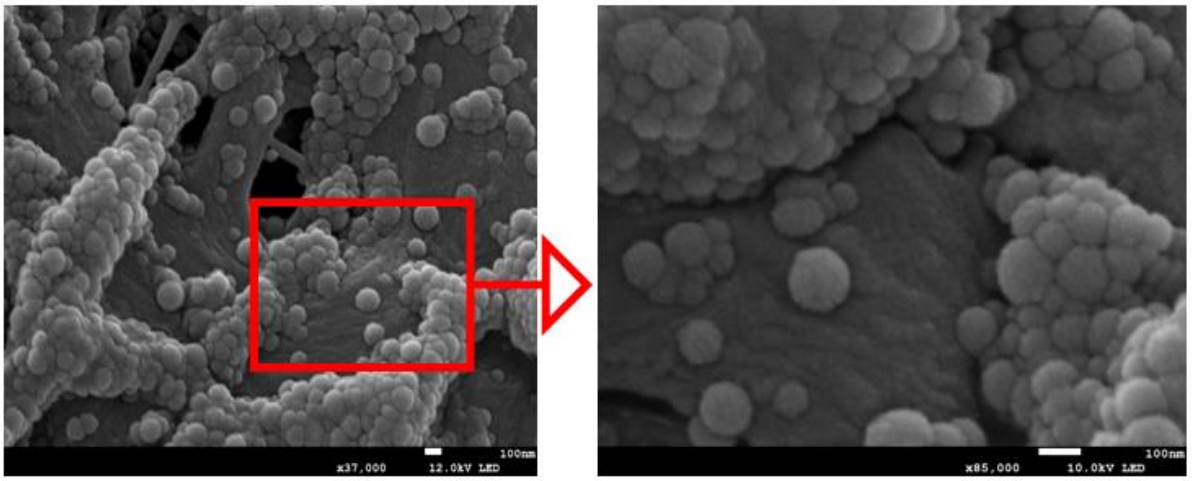

Figure 11: Cryo-SEM photographs of quercetin-loaded nanoparticles

To clearly understand the morphology and the adsorption of coating materials of the fabricated nanoparticles beyond Cryo-SEM photographs, TEM was carried out (*Figure 12*). The analyses of the TEM images confirmed that the particle size was less than 200nm. The photos showed that the core material (SH) was surrounded by stabilizers which were almond gum and T80. The results also showed no evidence of aggregation of the nanoparticles presenting the high stability of the particles.

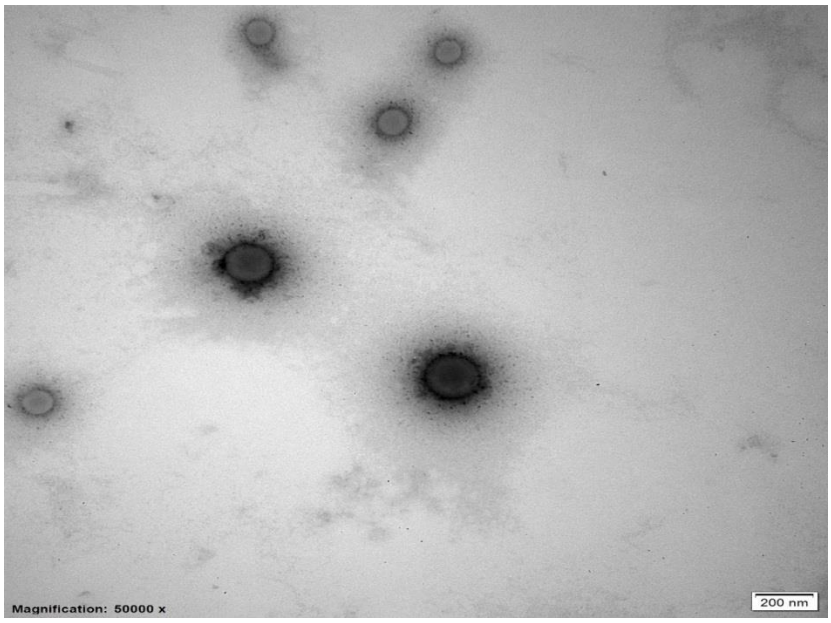

Figure 12: TEM photographs of quercetin-loaded nanoparticles

4.2.4 FTIR

FTIR is a very practical technique in studying the interactions between components. In this study, it was used to establish the interaction between quercetin and shellac in the nanoparticles. *Figure 13* shows the spectra for pure quercetin and shellac with quercetin particles without coating materials. In the spectrum for pure quercetin, there are three peaks marked in red with wavenumber of 815 cm^{-1} (C-H bend of aromatic hydrocarbon), 1516 cm^{-1} (C=O aromatic stretch) and 1612 cm^{-1} (C-C aromatic ring stretch) (Sambandam *et al*., 2016). However, these peaks were not observed in the spectrum for shellac and quercetin. This implies that at these points there is an interaction between shellac and quercetin. Li *et al*., (2014) reported that a reduction of the FTIR spectrum intensity in the similar points represents the interaction of quercetin with the studied compound.

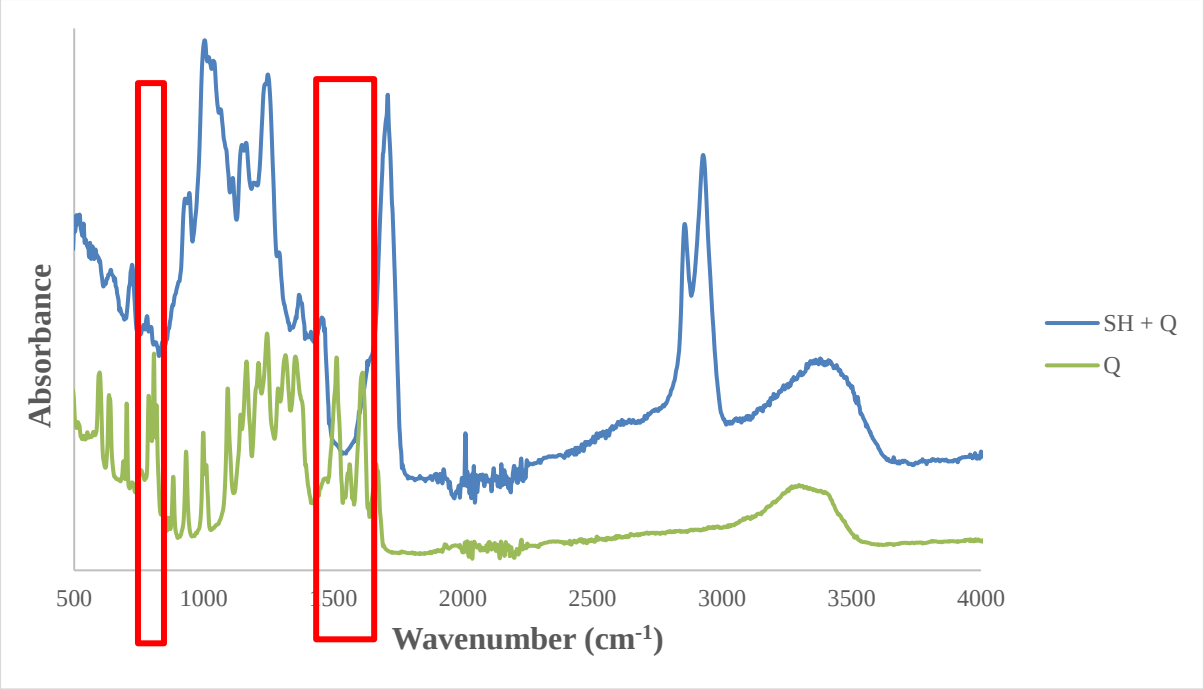

Figure 13: FTIR spectra of pure quercetin (green) and quercetin-shellac nanoparticles (blue)

4.4 Functionality and *in-vitro* properties

4.3.1 Redispersability

The nanoparticles may be applied to food products in dried form. Redispersibility therefore, helps to measure the ability of nanoparticles to properly be suspended in the digestive tract after being consumed. This ability can be measured by comparing the particle size before and after redispersion. The fabricated nanoparticles showed a good redispersability with no visible aggregation after redispersion. The average particle size before freeze-drying was 153.8±7.1nm and after redispersion, the size increased significantly to 172.9±1.4nm. However, the particle size was still small enough and within the acceptable range. This good redispersibility is attributed to the ability of AG to create a wall around the nanoparticles during dehydration and its ability to bind a lot of water during rehydration (Jooyandeh *et al*., 2017). There was also a significant increase in PDI from 0.254±0.032 before freeze-drying to 0.392±0.040 after redispersion. This further supports the fact that there was aggregation. However, a polydispersity index of 0.392 is still very acceptable implying that the aggregation was mild. *Figure 14* shows the particle size distribution variation before drying and after redispersion. It is obvious that the particle size distribution after redispersion is wider, but all the particles were in the nanometer range confirming that the fabricated nanoparticles had a good redispersability.

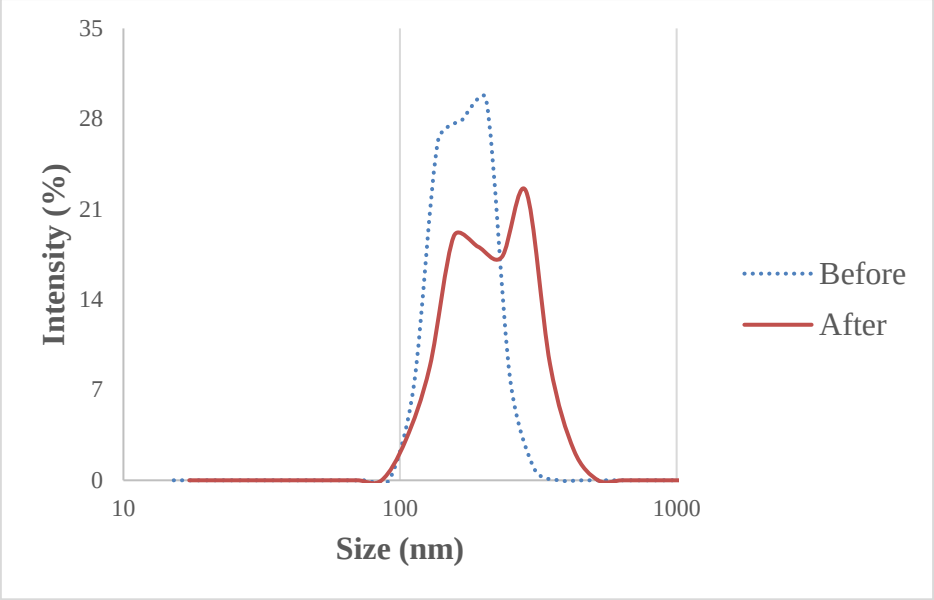

Figure 14: Particle size distribution for freshly prepared quercetin-loaded nanoparticles before freeze-drying (blue) and after redispersion of the freeze-dried nanoparticles (red)

4.3.2 Antioxidant activity

Figure 15 shows the antioxidant activity of quercetin in different GIT conditions. From time 0 to 120 min, it was in stomach conditions (pH 1.2) and from time 120 to 240 min, it was in intestinal conditions (pH 7.4). From the results, plain nanoparticles (without quercetin) showed almost no antioxidant activity in both conditions as it was expected. This means that all the antioxidant effect exhibited by the quercetin-loaded nanoparticles was due to the added quercetin. Therefore, SH, AG and T80 had no antioxidant activity. At pH 1.2, the antioxidant activity of free quercetin was around 200µM ascorbic acid equivalent throughout and was lower than the antioxidant activity of quercetin-loaded nanoparticles under the same conditions. Theoretically, the antioxidant activity of free quercetin is expected to be lower than that of quercetin-loaded nanoparticles at pH 1.2. This is because for quercetin-loaded nanoparticles at this pH, most of the quercetin is still entrapped in the nanoparticles and therefore not accessible. The higher antioxidant activity of quercetin-loaded nanoparticles is attributed to the high solubility of quercetin in the nanoparticles which is in amorphous form which easily diffuses out of the nanoparticles. Also, after two hours at pH 1.2, free quercetin was observed to aggregate (*Figure 16*), this might have also lowered its antioxidant activity. This implies that the antioxidant activity of quercetin was hampered by the low solubility at this pH. The antioxidant activity of quercetin-loaded nanoparticles was observed to increase very slightly with time at pH 1.2, this increase was not statistically significant, nonetheless. This slight increase may be due to the small release of amorphous quercetin from the core

material. This explanation may be taken into consideration for relatively high antioxidant activity of the nanoparticles at pH 1.2.

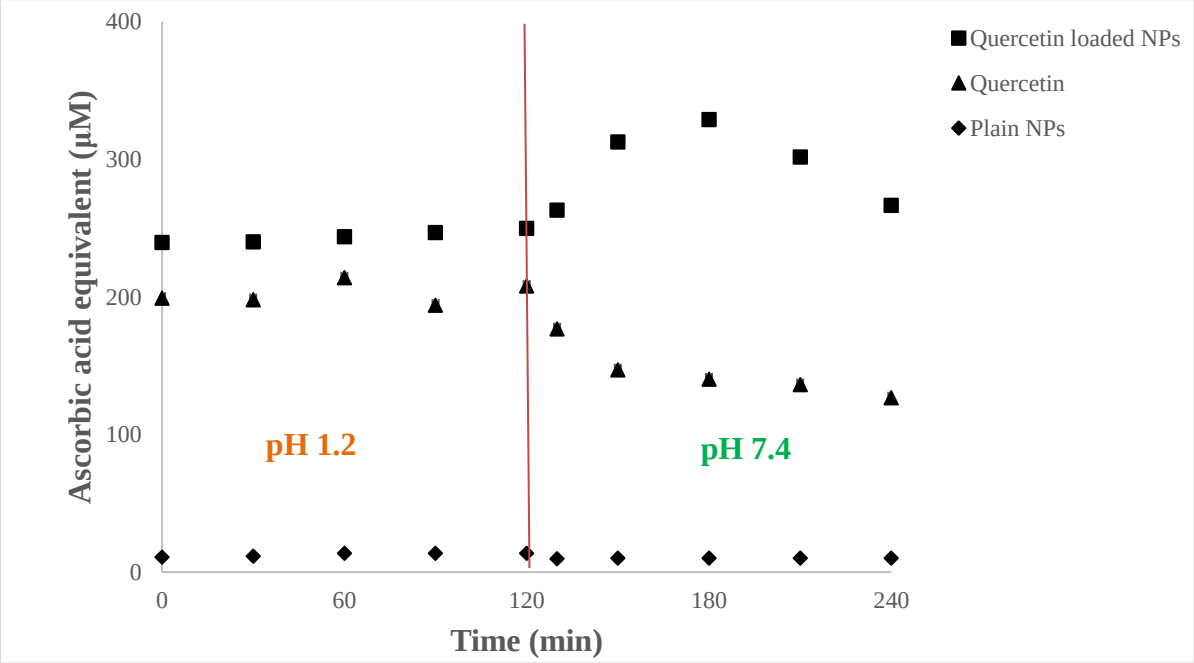

Figure 15: Antioxidant activity of quercetin-loaded nanoparticles, pure quercetin and plain nanoparticles (without Q) at pH 1.2 (stomach PH) and at pH 7.4 (intestinal pH). The vertical red line separates pH 1.2 from pH 7.4

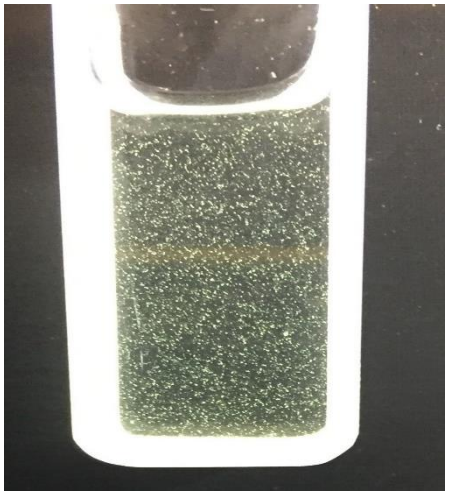

Figure 16: Aggregation of free quercetin at pH 1.2

At pH 7.4 (*Figure 17*), there was an immediate reduction in the antioxidant activity of free quercetin, which kept on reducing until the end of the experiment. The reduction in antioxidant activity was related to the degradation of quercetin at pH > 7. The degradation of quercetin at

alkaline pH has been extensively investigated (Buchner *et al*, 2006; Young Moon *et al*, 2008). However, for quercetin-loaded nanoparticles, an increase in antioxidant activity was observed which peaked after one hour from the time the pH was increased to 7.4. This enhanced and sustained antioxidant activity was due to the continuous release of quercetin from the nanoparticles due to the dissolution of shellac at alkaline pH (Patel *et al*., 2011). Indeed, the quercetin encapsulated within the nanoparticles core material could be protected from the alkaline conditions against degradation. Beyond the first hour, a rapid decrease in antioxidant activity was observed which is similar in trend to that of free quercetin. This was because most probably the major fraction of shellac has been dissolved and therefore all the quercetin is released which accelerates its degradation. It should, however, be noted that at the end of two hours in alkaline medium, the antioxidant activity of quercetin-loaded nanoparticles was still significantly higher than that of free quercetin. This was confirmed in Figure 17 showing the full absorbance spectrum of free quercetin and nanoparticles fortified by quercetin after 4h at pH 7.4. It was clear that free quercetin at pH 7.4 after 4h had a substantially lower absorbance peak around 380 nm as compared to the encapsulated quercetin in the similar medium, which is an indication of faster degradation of free quercetin. Therefore, it can be concluded that quercetin fortified nanoparticles offer a higher antioxidant activity than free quercetin. Wu *et al*. (2008), also reported quercetin-loaded nanoparticles to have a higher antioxidant activity than pure quercetin.

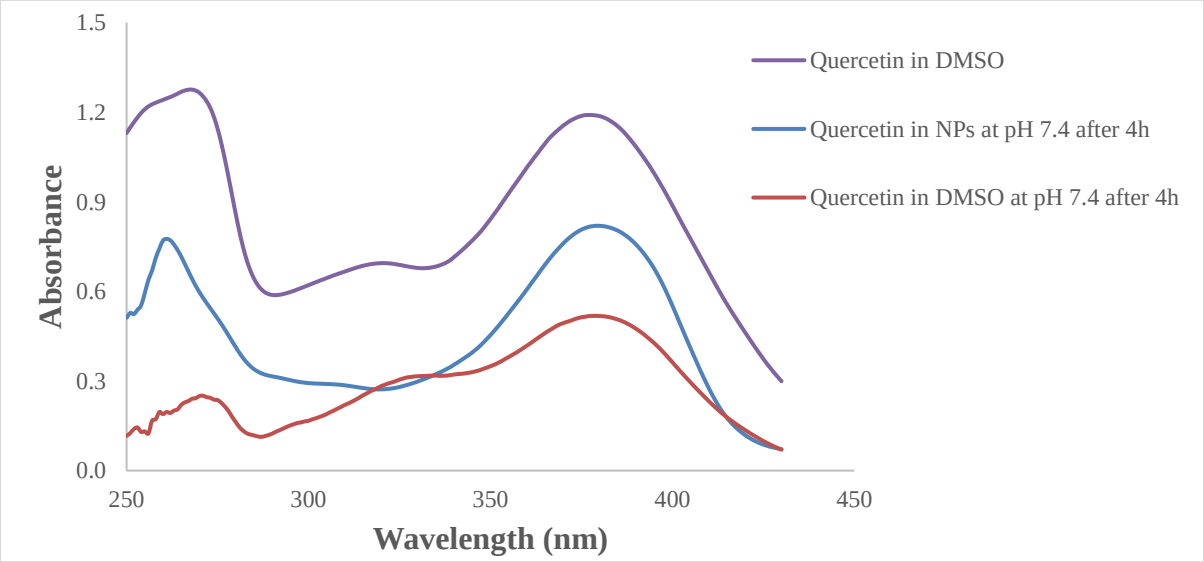

Figure 17: UV-Vis. spectra of quercetin in DMSO (purple), quercetin in nanoparticles (blue) and quercetin in DMSO at pH 7.4 (red) after 4 hours at 37°C

4.3.3 Cellular quantification of quercetin levels using Caco-2 cells

4.3.3.1 MTT and SRB

MTT assay is used to assess the cell metabolic activity while the SRB assay is used for the determination of the cell density through determination of cellular protein. Together, these two assays are used to assess the cytotoxicity of substances. The study of toxicity is very relevant in understanding the dynamics in the absorption of a bioactive compound. If the cells are damaged due to the presence of a toxic substance in the nanoparticles, it will lead to the impairment in the absorption of the bioactive compound. From *Figure 18*, the untreated sample is used as the reference. Results show that there was cell proliferation for only the sample treated with quercetin in DMSO while cells treated with DMSO without quercetin exhibited reactivity but without toxicity. In all the samples treated with nanoparticles, there was toxicity observed. The toxicity decreased with an increase in dilution and presence of quercetin. No significant toxicity was exhibited by cells treated with quercetin-loaded nanoparticles with a dilution factor of 100. Cells treated with quercetin-loaded nanoparticles exhibited less toxicity than those treated with nanoparticles with the same concentration but without quercetin. This implies that quercetin renders protection to cells against the toxic nanoparticles. This therefore confirms the protective function of quercetin. This cytoprotective effect of quercetin has also been well described by Gonzales *et al*. (2016). In their study, quercetin was shown to mitigate valinomycin-induced cellular stress. The decrease in toxicity with increase in dilution suggests that component(s) of the nanoparticles is responsible for this toxicity. According to the existing literature, T80 is expected to be the main contributor to this toxicity (Arechabala *et al*., 1999; Castro *et al*., 1995; Tsujino *et al*., 1999). These findings are in agreement with Manssens (2015), who studied the bioavailability of vitamin A in emulsions by in-vitro models. She clearly reports a decrease in toxicity of T80 stabilized emulsions with increase in dilution. Arechabala *et al*., (1999), reported the LC_{50} for T80 to be 210 μg/ml. However, according to our nanoparticles, a dilution factor of 50 led to a T80 concentration of 20 μg/ml while a dilution factor of 100 resulted into a concentration of 10μg/ml. These concentrations are lower than the reported $LC_{50,}$ but they are still significant enough to have toxic effects on the cells. This may also be due to the differentiation status of the cells, as undifferentiated, growing Caco-2 cells – such as used in this study - are more sensitive to toxicity in general compared to fully differentiated, enterocyte-like Caco-2 cells. This was for instance demonstrated by Rajkovic *et al*. (2014), who showed that exposure to the emetic toxin cereulide led to a 30-fold higher toxicity in undifferentiated cells compared to differentiated cells.

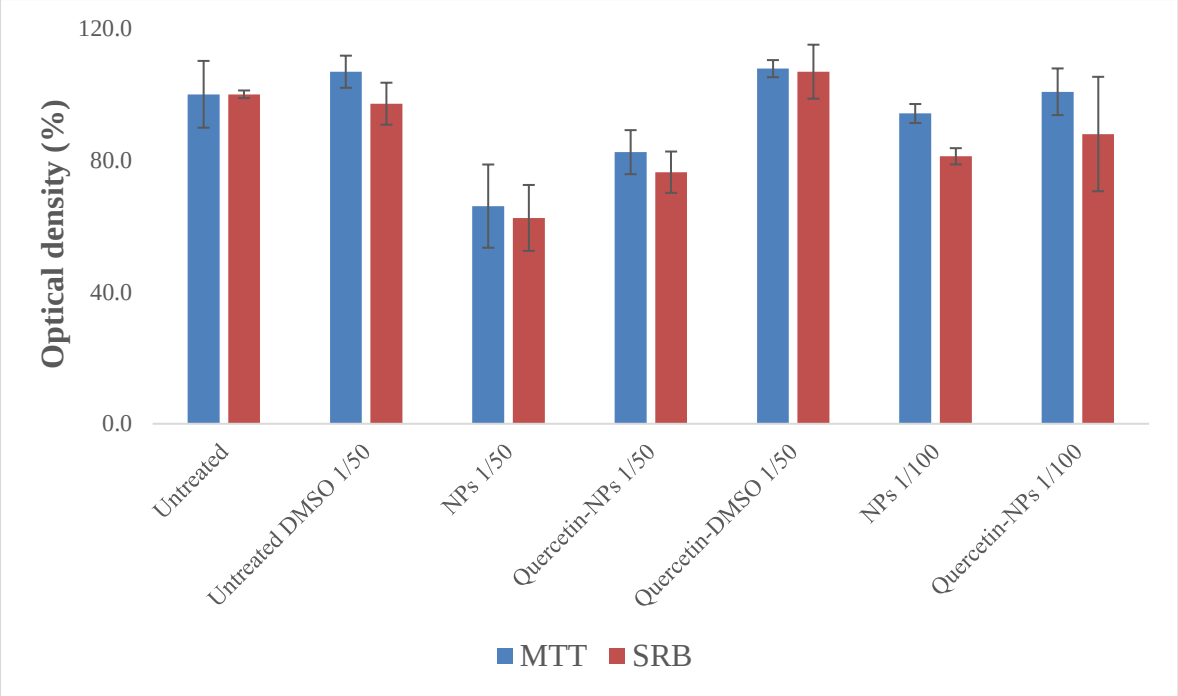

Figure 18: Results of the MTT (blue) and SRB (red) assays. The results are presented as a percentage of the optical density compared to the untreated cells

4.3.3.2 Absorption of quercetin

From *Figure 19*, cells treated with quercetin in DMSO significantly showed the highest absorption of quercetin followed by cells treated with quercetin-loaded nanoparticles with a dilution factor of 100. Cells treated with quercetin-loaded nanoparticles with a dilution factor of 50 had the lowest uptake of quercetin of the three different treatments containing quercetin. This trend in uptake of quercetin can be explained by the toxicity results presented above. Cells treated with quercetin in DMSO showed proliferation and therefore, their cell membranes were still very intact implying a normal uptake of quercetin. Cells treated with quercetin-loaded nanoparticles with a dilution factor of 100 showed a higher uptake of quercetin than those with a dilution factor of 50. This difference in uptake is because at lower dilution, the toxicity is high due high the concentration of T80 and therefore the integrity of the cell membrane is destroyed leading to impaired uptake of quercetin. At higher dilution, the toxicity is greatly reduced and the damage to the cell membrane is minimal. Even if quercetin concentration is also lower, the high integrity of the cell membrane allows for efficient absorption of quercetin. The average pH in the wall was 6.5-6.8. This was due to the acidification from the metabolically active cells. A pH below 7 has been shown to hinder the release of quercetin since shellac cannot fully solubilize (Leick *et al*., 2011). This therefore, might have led to less quercetin available for uptake by cells than what would have been available if the pH was 7.4.

Also at pH below 7, the degradation of quercetin is slowed down (Buchner *et al*., 2006; Young Moon *et al*., 2008). This implies that the amount of free quercetin that was available for uptake was higher than the amount that would have been available if the pH was 7.4. To correct for this pH difference and come up with actual luminal release, we calculated the area under the graphs of *Figure 15* at pH 7.4. From this calculation, it was found out that the amount of quercetin available for uptake from quercetin in DMSO was 47% of quercetin loaded in nanoparticles (100%). From this, we found out that the bioavailability of quercetin loaded in nanoparticles would have been much higher than free quercetin if the pH was maintained at 7.4. All the other treatments without quercetin showed no significant uptake of quercetin as expected.

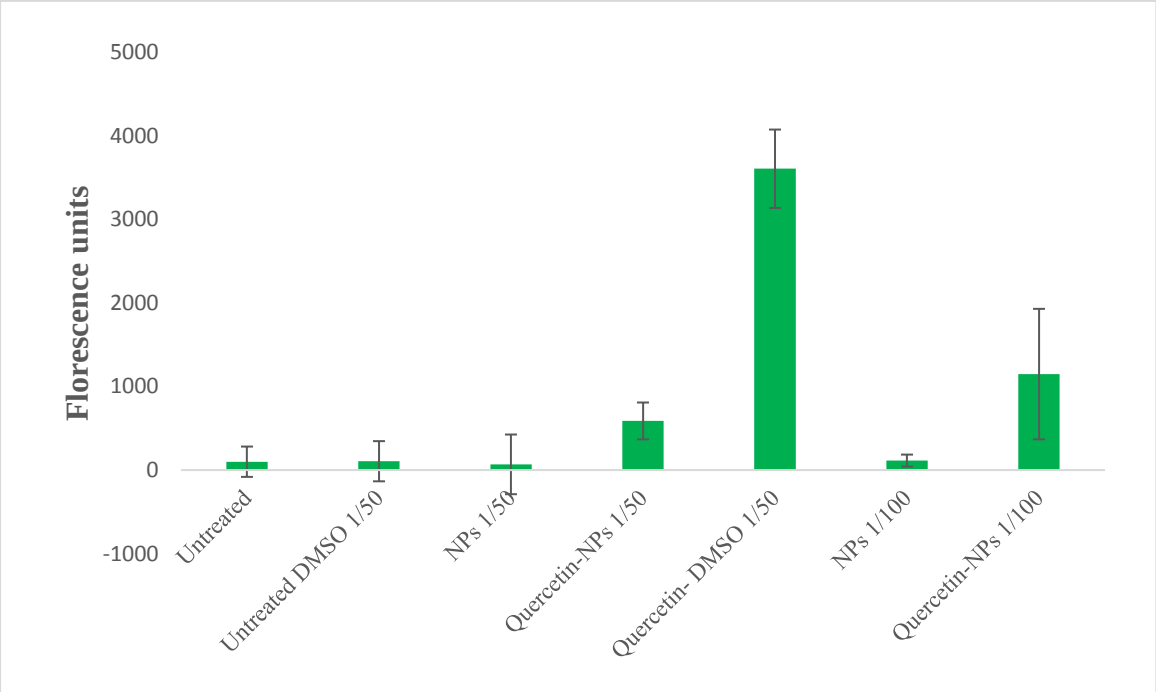

Figure 19: Results for uptake of quercetin by Caco-2 cells

4.4 Nutrition and development perspective

Worldwide, non-communicable diseases (NCDs) are responsible for 60% of the deaths of which 80% of these deaths are in developing countries. In Africa, the deaths from these diseases are rising faster than anywhere else in the world (WHO, 2010). Some of these diseases, such as some cancers, CVDs, and hypertension can be prevented by consuming diets that are rich in quercetin (Cossarizza *et al*., 2011; Dajas, 2012; Damianaki *et al*., 2000; Kuo, 1996; Park *et al*., 2005; Vijayababu *et al*., 2005; Wang *et al*., 2016). Therefore, incorporation of quercetin-loaded nanoparticles in food products can help to reduce this burden. There is a big connection

between reducing the disease burden and development: a healthy population can more easily escape from poverty compared to an unhealthy population (WHO, 2010). Production of food products containing quercetin-loaded nanoparticles especially in developing countries implies creating new jobs to the local communities in various sectors such as production, transportation and marketing. This will therefore help to improve the well-being of the people.

CHAPTER 5: CONCLUSION AND RECOMMENDATIONS

The antisolvent precipitation method was successfully capable to create coated nanoparticles with a relatively small particle size and high stability against acidic pH. It was discovered that a concentration of 0.1%w/v of T80 and 0.5%w/v of AG resulted into nanoparticles that were resistant against aggregation at pH 1.2. Quercetin-loaded nanoparticles with an average size of 135±8nm and a PDI of 0.252±0.01 were successfully produced. The encapsulation efficiency was 97.7±1.2%. These particles were found to be stable even at pH 1.2. Free quercetin is rapidly degraded at pH 7.4. However, when the quercetin was loaded in the nanoparticles, this degradation substantially decreased. The antioxidant activity of quercetin-loaded nanoparticles at pH 7.4 was found to be significantly higher that of free quercetin. The quercetin-loaded nanoparticles exhibited toxicity towards Caco-2 cells, which may be attributed to the presence of T80. T80 may have damaged the cell membrane of the cells, which hindered the uptake of quercetin by the Caco-2 cells. There is also evidence that quercetin may reduce the toxicity of the nanoparticles. Quercetin loaded in nanoparticles was found to be two times more available for absorption than free quercetin.

Further research is needed to develop quercetin-loaded nanoparticles without T80 to eliminate its toxic effects. More studies are also needed to eliminate completely T80 in food products due to its toxicity.

REFERENCES

Aditya, N. P., Macedo, A. S., Doktorovova, S., Souto, E. B., Kim, S., Chang, P. S., & Ko, S. (2014). Development and evaluation of lipid nanocarriers for quercetin delivery: A comparative study of solid lipid nanoparticles (SLN), nanostructured lipid carriers (NLC), and lipid nanoemulsions (LNE). *LWT - Food Science and Technology*, *59*(1), 115–121. https://doi.org/10.1016/j.lwt.2014.04.058

Arechabala, B., Coiffard, C., Rivalland, P., Coiffard, L. J. M., & De Roeck-Holtzhauer, Y. (1999). Comparison of cytotoxicity of various surfactants tested on normal human fibroblast cultures using the neutral red test, MTT assay and LDH release. *Journal of Applied Toxicology*, *19*(3), 163–165. https://doi.org/10.1002/(SICI)1099-1263(199905/06)19:3<163::AID-JAT561>3.0.CO;2-H

Arts, M. J. T. ., Sebastiaan Dallinga, J., Voss, H.-P., Haenen, G. R. M. ., & Bast, A. (2004). A new approach to assess the total antioxidant capacity using the TEAC assay. *Food Chemistry*, *88*(4), 567–570. https://doi.org/10.1016/j.foodchem.2004.02.008

Asasutjarit, R., Sorrachaitawatwong, C., Tipchuwong, N., & Pouthai, S. (2013). Effect of formulation compositions on particle size and zeta potential of diclofenac sodium-loaded chitosan nanoparticles. *International Journal of Medical, Health, Biomedical, Bioengineering, and Pharmaceutical Engineering*, *7*(9), 309–311.

Awad, H. M., Boersma, M. G., Boeren, S., Van Bladeren, P. J., Vervoort, J., & Rietjens, I. M. C. M. (2002). The regioselectivity of glutathione adduct formation with flavonoid quinone/quinone methides is pH-dependent. *Chemical Research in Toxicology*, *15*(3), 343–351. https://doi.org/10.1021/tx010132l

Bagad, M., & Khan, A. Z. (2015). Poly (n - butylcyanoacrylate) nanoparticles for oral delivery of quercetin : preparation , characterization , and pharmacokinetics and biodistribution studies in Wistar rats. *International Journal of Nanomedicine*, 1–12.

Baghel, S. S., Shrivastava, N., Baghel, R. S., & Rajput, S. (2012). a Review of Quercetin : Antioxidant and Anticancer Properties. *World Journal of Pharmacy and Pharmaceutical Sciences*, *1*(1), 146–160.

Baḱldyga, J., Podgórska, W., & Pohorecki, R. (1995). Mixing-precipitation model with application to double feed semibatch precipitation. *Chemical Engineering Science*, *50*(8),

1281–1300. https://doi.org/10.1016/0009-2509(95)98841-2

Bala, I., Bhardwaj, V., Hariharan, S., Kharade, S. V., Roy, N., & Kumar, M. N. V. R. (2006). Sustained release nanoparticulate formulation containing antioxidant-ellagic acid as potential prophylaxis system for oral administration. *Journal of Drug Targeting*, *14*(1), 27–34. https://doi.org/10.1080/10611860600565987

Bałdyga, J., Bourne, J. R., & Hearn, S. J. (1997). Interaction between chemical reactions and mixing on various scales. *Chemical Engineering Science*, *52*(4), 457–466. https://doi.org/10.1016/S0009-2509(96)00430-7

Barrett, M., O'Grady, D., Casey, E., & Glennon, B. (2011). The role of meso-mixing in anti-solvent crystallization processes. *Chemical Engineering Science*, *66*(12), 2523–2534. https://doi.org/10.1016/j.ces.2011.02.042

Bhalekar, M. R., Pokharkar, V., Madgulkar, A., Patil, N., & Patil, N. (2009). Preparation and Evaluation of Miconazole Nitrate-Loaded Solid Lipid Nanoparticles for Topical Delivery. *AAPS PharmSciTech*, *10*(1), 289–296. https://doi.org/10.1208/s12249-009-9199-0

Bhatia, S. (2016). *Natural polymer drug delivery systems: Nanoparticles, plants, and algae. Springer International Publishing Switzerland*. https://doi.org/10.1007/978-3-319-41129-3

Biasutto, L., Marotta, E., Garbisa, S., Zoratti, M., & Paradisi, C. (2010). Determination of quercetin and resveratrol in whole blood-implications for bioavailability studies. *Molecules*, *15*(9), 6570–6579. https://doi.org/10.3390/molecules15096570

Boots, A. W., Kubben, N., Haenen, G. R. M. M., & Bast, A. (2003). Oxidized quercetin reacts with thiols rather than with ascorbate: Implication for quercetin supplementation. *Biochemical and Biophysical Research Communications*, *308*(3), 560–565. https://doi.org/10.1016/S0006-291X(03)01438-4

Bose, S., & Michniak-Kohn, B. (2013). Preparation and characterization of lipid based nanosystems for topical delivery of quercetin. *European Journal of Pharmaceutical Sciences*, *48*(3), 442–452. https://doi.org/10.1016/j.ejps.2012.12.005

Bouaziz, F., Ben Romdhane, M., Boisset Helbert, C., Buon, L., Bhiri, F., Bardaa, S., … Ellouz Chaabouni, S. (2014). Healing efficiency of oligosaccharides generated from almond gum

(Prunus amygdalus) on dermal wounds of adult rats. *Journal of Tissue Viability*, *23*(3), 98–108. https://doi.org/10.1016/j.jtv.2014.07.001

Bouaziz, F., Helbert, C. B., Romdhane, M. Ben, Koubaa, M., Bhiri, F., Kallel, F., … Chaabouni, S. E. (2014). Structural data and biological properties of almond gum oligosaccharide: Application to beef meat preservation. *International Journal of Biological Macromolecules*, *72*, 472–479. https://doi.org/10.1016/j.ijbiomac.2014.08.044

Boudad, H., Legrand, P., Lebas, G., Cheron, M., Duchêne, D., & Ponchel, G. (2001). Combined hydroxypropyl-β-cyclodextrin and poly(alkylcyanoacrylate) nanoparticles intended for oral administration of saquinavir. *International Journal of Pharmaceutics*, *218*(1–2), 113–124. https://doi.org/10.1016/S0378-5173(01)00622-6

Brown, K. S. (1973). The chemistry of aphids and scale insects. *Chemical Society Reviews*, *4*(2), 263–288. https://doi.org/10.1039/cs9750400263

Buchner, N. Krumbein, A. Rohn, S. and Kroh, W. . (2006). Effect of thermal processing on the flavonols rutin and quercetin. *Rapid Communications in Mass Spectrometry : RCM*, *20*(20), 3229–3235. https://doi.org/10.1002/rcm

Castro, C. A., Hogan, J. B., Benson, K. A., Shehata, C. W., & Landauer, M. R. (1995). Behavioral effects of vehicles: DMSO, ethanol, Tween-20, Tween-80, and emulphor-620. *Pharmacology, Biochemistry and Behavior*, *50*(4), 521–526. https://doi.org/10.1016/0091-3057(94)00331-9

Comalada, M., Camuesco, D., Sierra, S., Ballester, I., Xaus, J., Gálvez, J., & Zarzuelo, A. (2005). In vivo quercitrin anti-inflammatory effect involves release of quercetin, which inhibits inflammation through down-regulation of the NF-κB pathway. *European Journal of Immunology*, *35*(2), 584–592. https://doi.org/10.1002/eji.200425778

Cossarizza, A., Gibellini, L., Pinti, M., Nasi, M., Montagna, J. P., De Biasi, S., … Cooper, E. L. (2011). Quercetin and cancer chemoprevention. *Evidence-Based Complementary and Alternative Medicine*, *2011*. https://doi.org/10.1093/ecam/neq053

Cui, L., Liu, Z. P., Yu, D. G., Zhang, S. P., Bligh, S. W. A., & Zhao, N. (2014). Electrosprayed core-shell nanoparticles of PVP and shellac for furnishing biphasic controlled release of ferulic acid. *Colloid and Polymer Science*, *292*(9), 2089–2096. https://doi.org/10.1007/s00396-014-3226-8

Dai, J., Nagai, T., Wang, X., Zhang, T., Meng, M., & Zhang, Q. (2004). PH-sensitive nanoparticles for improving the oral bioavailability of cyclosporine a. *International Journal of Pharmaceutics*, *280*(1–2), 229–240. https://doi.org/10.1016/j.ijpharm.2004.05.006

Dajas, F. (2012). Life or death: Neuroprotective and anticancer effects of quercetin. *Journal of Ethnopharmacology*, *143*(2), 383–396. https://doi.org/10.1016/j.jep.2012.07.005

Dalvi, S. V, & Dave, R. N. (2009). Controlling Particle Size of a Poorly Water-Soluble Drug Using Ultrasound and Stabilizers in Antisolvent Precipitation. *Society*, (3), 7581–7593.

Damianaki, A., Bakogeorgou, E., Kampa, M., Notas, G., Hatzoglou, A., Panagiotou, S., … Castanas, E. (2000). Potent inhibitory action of red wine polyphenols on human breast cancer cells. *J Cell Biochem*, *78*(3), 429–441. https://doi.org/10.1002/1097-4644(20000901)78:3<429::AID-JCB8>3.0.CO;2-M [pii]

Davidov-Pardo, G., Joye, I. J., & McClements, D. J. (2015). Encapsulation of resveratrol in biopolymer particles produced using liquid antisolvent precipitation. Part 1: Preparation and characterization. *Food Hydrocolloids*, *45*, 309–316. https://doi.org/10.1016/j.foodhyd.2014.11.023

De Paz, E., Martín, Á., Every, H., & Cocero, M. J. (2015). Production of water-soluble quercetin formulations by antisolvent precipitation and supercritical drying. *Journal of Supercritical Fluids*, *104*, 281–290. https://doi.org/10.1016/j.supflu.2015.07.006

Dinesh Kumar, V., Verma, P. R. P., & Singh, S. K. (2016). Morphological and in vitro antibacterial efficacy of quercetin loaded nanoparticles against food-borne microorganisms. *LWT - Food Science and Technology*, *66*, 638–650. https://doi.org/10.1016/j.lwt.2015.11.004

Doost, A. S., Rahadian, D., Muhammad, A., Stevens, C. V, & Meeren, P. Van Der. (2018). Fabrication and characterization of quercetin loaded almond gum-shellac nanoparticles prepared by antisolvent precipitation. *Food Hydrocolloids*. https://doi.org/10.1016/j.foodhyd.2018.04.050

Farag, Y., & Leopold, C. S. (2009). Physicochemical properties of various shellac types. *Dissolution Technologies*, *16*(2), 33–39. https://doi.org/10.1691/ph.2008.7308

Fessi, H., Puisieux, F., Devissaguet, J. P., Ammoury, N., & Benita, S. (1989). Nanocapsule formation by interfacial polymer deposition following solvent displacement. *International Journal of Pharmaceutics*, *55*(1), 1–4. https://doi.org/10.1016/0378-5173(89)90281-0

Food Safety Commission. (2007). Evaluation Report of Food Additives Polysorbates. *Food Safety Commission Japan*, (June).

Gao, L., Liu, G., Wang, X., Liu, F., Xu, Y., & Ma, J. (2011). Preparation of a chemically stable quercetin formulation using nanosuspension technology. *International Journal of Pharmaceutics*, *404*(1–2), 231–237. https://doi.org/10.1016/j.ijpharm.2010.11.009

Goldberg, D. M., Yan, J., & Soleas, G. J. (2003). Absorption of three wine-related polyphenols in three different matrices by healthy subjects. *Clinical Biochemistry*, *36*(1), 79–87. https://doi.org/10.1016/S0009-9120(02)00397-1

Gonzales, G. B., Smagghe, G., Vissenaekens, H., Grootaert, C., Rajkovic, A., Van de Wiele, T., … Van Camp, J. (2016). Quercetin mitigates valinomycin-induced cellular stress via stress-induced metabolism and cell uptake. *Molecular Nutrition and Food Research*, *60*(5), 972–980. https://doi.org/10.1002/mnfr.201500999

Grootaert, C., Gonzales, G. B., Vissenaekens, H., Van De Wiele, T., Raes, K., Smagghe, G., & Van Camp, J. (2016). Flow Cytometric Method for the Detection of Flavonoids in Cell Lines. *Journal of Biomolecular Screening*, *21*(8), 858–865. https://doi.org/10.1177/1087057116653220

Igual, M., García-Martínez, E., Camacho, M. M., & Martínez-Navarrete, N. (2011). Changes in flavonoid content of grapefruit juice caused by thermal treatment and storage. *Innovative Food Science and Emerging Technologies*, *12*(2), 153–162. https://doi.org/10.1016/j.ifset.2010.12.010

Jacobs, C., Kayser, O., & Muller, H. . (2000). Nanosuspensions as a new approach for the formulation for the poorly soluble drug tarazepide. *International Journal of Pharmaceutics*, *196*, 161–164. https://doi.org/10.2174/157341309789378177

Jooyandeh, H., Goudarzi, M., Rostamabadi, H., & Hojjati, M. (2017). Effect of Persian and almond gums as fat replacers on the physicochemical, rheological, and microstructural attributes of low-fat Iranian White cheese. *Food Science and Nutrition*, *5*(3), 669–677. https://doi.org/10.1002/fsn3.446

Joye, I. J., & McClements, D. J. (2013). Production of nanoparticles by anti-solvent precipitation for use in food systems. *Trends in Food Science and Technology*, *34*(2), 109–123. https://doi.org/10.1016/j.tifs.2013.10.002

Kakran, M., Sahoo, N. G., Li, L., & Judeh, Z. (2012). Fabrication of quercetin nanoparticles by anti-solvent precipitation method for enhanced dissolution. *Powder Technology*, *223*, 59–64. https://doi.org/10.1016/j.powtec.2011.08.021

Kakran, M., Sahoo, N. G., Tan, I. L., & Li, L. (2012). Preparation of nanoparticles of poorly water-soluble antioxidant curcumin by antisolvent precipitation methods. *Journal of Nanoparticle Research*, *14*(3). https://doi.org/10.1007/s11051-012-0757-0

Kerem, Z., Bravdo, B. A., Shoseyov, O., & Tugendhaft, Y. (2004). Rapid liquid chromatography-ultraviolet determination of organic acids and phenolic compounds in red wine and must. *Journal of Chromatography A*, *1052*(1–2), 211–215. https://doi.org/10.1016/j.chroma.2004.08.105

Khan, S. A., & Schneider, M. (2013). Improvement of Nanoprecipitation Technique for Preparation of Gelatin Nanoparticles and Potential Macromolecular Drug Loading. *Macromolecular Bioscience*, *13*(4), 455–463. https://doi.org/10.1002/mabi.201200382

Khorram, F., Ramezanian, A., & Hosseini, S. M. H. (2017). Shellac, gelatin and Persian gum as alternative coating for orange fruit. *Scientia Horticulturae*, *225*(July), 22–28. https://doi.org/10.1016/j.scienta.2017.06.045

Kim, B. H., Choi, J. S., Yi, E. H., Lee, J. K., Won, C., Ye, S. K., & Kim, M. H. (2013). Relative antioxidant activities of quercetin and its structurally related substances and their effects on NF-κB/CRE/AP-1 signaling in murine macrophages. *Molecules and Cells*, *35*(5), 410–420. https://doi.org/10.1007/s10059-013-0031-z

Kim, S., Ng, W. K., Dong, Y., Das, S., & Tan, R. B. H. (2012). Preparation and physicochemical characterization of trans-resveratrol nanoparticles by temperature-controlled antisolvent precipitation. *Journal of Food Engineering*, *108*(1), 37–42. https://doi.org/10.1016/j.jfoodeng.2011.07.034

Kraisit, P., Limmatvapirat, S., Nunthanid, J., Sriamornsak, P., & Luangtana-anan, M. (2013). Nanoparticle formation by using shellac and chitosan for a protein delivery system. *Pharmaceutical Development and Technology*, *18*(3), 686–93.

https://doi.org/10.3109/10837450.2012.685657

Kukongviriyapan, U., Sompamit, K., Pannangpetch, P., Kukongviriyapan, V., & Donpunha, W. (2012). Preventive and therapeutic effects of quercetin on lipopolysaccharide-induced oxidative stress and vascular dysfunction in mice. *Canadian Journal of Physiology and Pharmacology*, *90*(10), 1345–1353. https://doi.org/10.1139/y2012-101

Kuo, S.-M. (1996). Antiproliferative potency of structurally distinct dietary flavonoids on human colon cancer cells. *Cancer Letters*, *110*, *41-48*.

Ladizinsky, G. (1999). On the origin of almond gum. *Generic Resourses and Crop Evaluation*, *46*, 143–147.

Langer, K., Balthasar, S., Vogel, V., Dinauer, N., Von Briesen, H., & Schubert, D. (2003). Optimization of the preparation process for human serum albumin (HSA) nanoparticles. *International Journal of Pharmaceutics*, *257*(1–2), 169–180. https://doi.org/10.1016/S0378-5173(03)00134-0

Lee, J. H., Kim, Y., Hoang, M. H., Jun, H. jin, & Lee, S. J. (2014). Rapid quantification of cellular flavonoid levels using quercetin and a fluorescent diphenylboric acid 2-amino ethyl ester probe. *Food Science and Biotechnology*, *23*(1), 75–79. https://doi.org/10.1007/s10068-014-0010-y

Leick, S., Kott, M., Degen, P., Henning, S., Päsler, T., Suter, D., & Rehage, H. (2011). Mechanical properties of liquid-filled shellac composite capsules. *Phys. Chem. Chem. Phys.*, *13*(7), 2765–2773. https://doi.org/10.1039/C0CP01803A

Li, C., Yu, D. G., Williams, G. R., & Wang, Z. H. (2014). Fast-dissolving core-shell composite microparticles of quercetin fabricated using a coaxial electrospray process. *PLoS ONE*, *9*(3). https://doi.org/10.1371/journal.pone.0092106

Luangaram, S., Kukongviriyapan, U., Pakdeechote, P., Kukongviriyapan, V., & Pannangpetch, P. (2007). Protective effects of quercetin against phenylhydrazine-induced vascular dysfunction and oxidative stress in rats. *Food and Chemical Toxicology*, *45*(3), 448–455. https://doi.org/10.1016/j.fct.2006.09.008

Lyczko, N., Espitalier, F., Louisnard, O., & Schwartzentruber, J. (2002). Effect of ultrasound on the induction time and the metastable zone widths of potassium sulphate. *Chemical*

Engineering Journal, *86*(3), 233–241. https://doi.org/10.1016/S1385-8947(01)00164-4

Ma, K., Qiu, Y., Fu, Y., & Ni, Q.-Q. (2017). Improved shellac mediated nanoscale application drug release effect in a gastric-site drug delivery system. *RSC Advances*, *7*(84), 53401–53406. https://doi.org/10.1039/C7RA10757A

Mahfoudhi, N., Chouaibi, M., & Hamdi, S. (2013). Effectiveness of almond gum trees exudate as a novel edible coating for improving postharvest quality of tomato (Solanum lycopersicum L.) fruits. *Food Science and Technology International = Ciencia y Tecnologia de Los Alimentos Internacional*, (January). https://doi.org/10.1177/1082013212469617

Mahfoudhi, N., & Hamdi, S. (2015a). Kinetic Degradation and Storage Stability of β-Carotene Encapsulated by Freeze-Drying Using Almond Gum and Gum Arabic as Wall Materials. *Journal of Food Processing and Preservation*, *39*(6), 896–906. https://doi.org/10.1111/jfpp.12302

Mahfoudhi, N., & Hamdi, S. (2015b). Use of Almond Gum and Gum Arabic as Novel Edible Coating to Delay Postharvest Ripening and to Maintain Sweet Cherry (Prunus avium) Quality during Storage. *Journal of Food Processing and Preservation*, *39*(6), 1499–1508. https://doi.org/10.1111/jfpp.12369

Mahfoudhi, N., Sessa, M., Chouaibi, M., Ferrari, G., Donsì, F., & Hamdi, S. (2014). Assessment of emulsifying ability of almond gum in comparison with gum arabic using response surface methodology. *Food Hydrocolloids*, *37*, 49–59. https://doi.org/10.1016/j.foodhyd.2013.10.009

Manssens, H. (2015). Study of vitamin A bioavailability by in vitro models (Master's dessertation). *Faculty of Bioscience Engineering, Universiteit Gent*.

Matteucci, M. E., Hotze, M. A., Johnston, K. P., & Williams, R. O. (2006). Drug nanoparticles by antisolvent precipitation: Mixing energy versus surfactant stabilization. *Langmuir*, *22*(21), 8951–8959. https://doi.org/10.1021/la061122t

Meer, T. A., Sawant, K. P., & Amin, P. D. (2011). Liquid antisolvent precipitation process for solubility modulation of bicalutamide. *Acta Pharmaceutica*, *61*(4), 435–445. https://doi.org/10.2478/v10007-011-0036-0

Müller, R. H., Rühl, D., Runge, S., Schulze-Forster, K., & Mehnert, W. (1997). Cytotoxicity of solid lipid nanoparticles as a function of the lipid matrix and the surfactant. *Pharmaceutical Research*. https://doi.org/10.1023/A:1012043315093

Murakami, H., Kobayashi, M., Takeuchi, H., & Kawashima, Y. (1999). Preparation of poly(DL-lactide-co-glycolide) nanoparticles by modified spontaneous emulsification solvent diffusion method. *International Journal of Pharmaceutics*, *187*(2), 143–152. https://doi.org/10.1016/S0378-5173(99)00187-8

Park, C. H., Chang, J. Y., Hahm, E. R., Park, S., Kim, H. K., & Yang, C. H. (2005). Quercetin, a potent inhibitor against β-catenin/Tcf signaling in SW480 colon cancer cells. *Biochemical and Biophysical Research Communications*, *328*(1), 227–234. https://doi.org/10.1016/j.bbrc.2004.12.151

Park, S. J., Jeon, S. Y., & Yeo, S. Do. (2006). Recrystallization of a pharmaceutical compound using liquid and supercritical antisolvents. *Industrial and Engineering Chemistry Research*, *45*(7), 2287–2293. https://doi.org/10.1021/ie0510775

Patel, A., Heussen, P., Hazekamp, J., & Velikov, K. P. (2011). Stabilisation and controlled release of silibinin from pH responsive shellac colloidal particles. *Soft Matter*, *7*(18), 8549. https://doi.org/10.1039/c1sm05853c

Patel, A. R., Remijn, C., Cabero, A. I. M., Heussen, P. C. M., Ten Hoorn, J. W. M. S., & Velikov, K. P. (2013). Novel all-natural microcapsules from gelatin and shellac for biorelated applications. *Advanced Functional Materials*, *23*(37), 4710–4718. https://doi.org/10.1002/adfm.201300320

Pogorzelski, S., Watrobska-swietlikowska, D., & Sznitowska, M. (2012). Surface tensometry studies on formulations of surfactants with preservatives as a tool for antimicrobial drug protection characterization. *Journal of Biophysical Chemisrty*, *3*(4), 324–333.

Priprem, A., Watanatorn, J., Sutthiparinyanont, S., Phachonpai, W., & Muchimapura, S. (2008). Anxiety and cognitive effects of quercetin liposomes in rats. *Nanomedicine: Nanotechnology, Biology, and Medicine*, *4*(1), 70–78. https://doi.org/10.1016/j.nano.2007.12.001

Rajkovic, A., Grootaert, C., Butorac, A., Cucu, T., De Meulenaer, B., van Camp, J., … Cindrić, M. (2014). Sub-emetic toxicity of Bacillus cereus toxin cereulide on cultured human

enterocyte-like Caco-2 cells. *Toxins*, *6*(8), 2270–2290. https://doi.org/10.3390/toxins6082270

Ranilla, L. G., Genovese, M. I., & Lajolo, F. M. (2009). Effect of different cooking conditions on phenolic compounds and antioxidant capacity of some selected Brazilian bean (Phaseolus vulgaris L.) cultivars. *Journal of Agricultural and Food Chemistry*, *57*(13), 5734–5742. https://doi.org/10.1021/jf900527v

Ravichandran, R., Rajendran, M., & Devapiriam, D. (2014). Antioxidant study of quercetin and their metal complex and determination of stability constant by spectrophotometry method. *Food Chemistry*, *146*, 472–478. https://doi.org/10.1016/j.foodchem.2013.09.080

Rezaei, A., Nasirpour, A., & Tavanai, H. (2016). Fractionation and some physicochemical properties of almond gum (Amygdalus communis L.) exudates. *Food Hydrocolloids*, *60*, 461–469. https://doi.org/10.1016/j.foodhyd.2016.04.027

Rezaei, A., Tavanai, H., & Nasirpour, A. (2016). Fabrication of electrospun almond gum/PVA nanofibers as a thermostable delivery system for vanillin. *International Journal of Biological Macromolecules*, *91*, 536–543. https://doi.org/10.1016/j.ijbiomac.2016.06.005

Roda, A., Simoni, P., Magliulo, M., Nanni, P., Baraldini, M., Roda, G., & Roda, E. (2007). A new oral formulation for the release of sodium butyrate in the ileo-cecal region and colon. *World Journal of Gastroenterology*, *13*(7), 1079–1084.

Ruma, K., Sunil, K., & Prakash, H. S. (2013). Antioxidant, anti-inflammatory, antimicrobial and cytotoxic properties of fungal endophytes from Garcinia species. *International Journal of Pharmacy and Pharmaceutical Sciences*, *5*(SUPPL 3), 889–897.

Sambandam, B., Thiyagarajan, D., Ayyaswamy, A., & Raman, P. (2016). Extraction and isolation of flavonoid quercetin from the leaves of Trigonella foenum-graecum and their anti-oxidant activity. *International Journal of Pharmacy and Pharmaceutical Sciences*, *8*(6), 120–124.

Schroeter, H., Boyd, C., Spencer, J. P. E., Williams, R. J., Cadenas, E., & Rice-evans, C. (2002). MAPK signaling in neurodegeneration : influences of flavonoids and of nitric oxide. *Neurobiology of Aging*, *23*, 861–880.

Sedaghat Doost, A., Muhammad, D. R. A., Stevens, C. V, Dewettinck, K., & Van der Meeren,

P. (2018). Fabrication and characterization of quercetin loaded almond gum-shellac nanoparticles prepared by antisolvent precipitation. *Food Hydrocolloids*, *83*, 190–201. https://doi.org/https://doi.org/10.1016/j.foodhyd.2018.04.050

Selvasudha, N., & Koumaravelou, K. (2017). The multifunctional synergistic effect of chitosan on simvastatin loaded nanoparticulate drug delivery system. *Carbohydrate Polymers*, *163*, 70–80. https://doi.org/10.1016/j.carbpol.2017.01.038

Sheorey, D. S., Shastri, A. S., & Dorle, A. K. (1991). Effect of variables on the preparation of shellac microcapsules by solvent evaporation technique: Part 1. *International Journal of Pharmaceutics*, *68*(1–3), 19–23. https://doi.org/10.1016/0378-5173(91)90122-5

Skaper, S. D., Fabris, M., Ferrari, V., Carbonare, M. D., & Leon, A. (1997). Including Sensory Neurons From Oxidative Stress Induced By Glutathione Depletion : Cooperative Effects of Ascorbic Acid. *Free Radidical Biology & Medicine*, *22*(4), 669–678.

Sukmawati, A., Utami, W., Yuliani, R., Da'i, M., & Nafarin, A. (2018). Effect of tween 80 on nanoparticle preparation of modified chitosan for targeted delivery of combination doxorubicin and curcumin analogue. *IOP Conference Series: Materials Science and Engineering*, *311*, 012024. https://doi.org/10.1088/1757-899X/311/1/012024

Sun, C., Xu, C., Mao, L., Wang, D., Yang, J., & Gao, Y. (2017). Preparation, characterization and stability of curcumin-loaded zein-shellac composite colloidal particles. *Food Chemistry*, *228*, 656–667. https://doi.org/10.1016/j.foodchem.2017.02.001

Syed Ahamed Hussain, I., & Jaisankar, V. (2017). An eco-friendly synthesis, characterization and antibacterial applications of novel almond gum – poly(acrylamide) based hydrogel silver nanocomposite. *Polymer Testing*, *62*, 154–161. https://doi.org/10.1016/j.polymertesting.2017.06.021

Tan, Q., Liu, W., Guo, C., & Zhai, G. (2011). Preparation and evaluation of quercetin-loaded lecithin-chitosan nanoparticles for topical delivery. *International Journal of Nanomedicine*, *6*, 1621–1630. https://doi.org/10.2147/IJN.S22411

Thorat, A. A., & Dalvi, S. V. (2012). Liquid antisolvent precipitation and stabilization of nanoparticles of poorly water soluble drugs in aqueous suspensions: Recent developments and future perspective. *Chemical Engineering Journal*, *181–182*, 1–34. https://doi.org/10.1016/j.cej.2011.12.044

Tsujino, I., Yamazaki, T., Masutani, M., Sawada, U., & Horie, T. (1999). Effect of Tween-80 on cell killing by etoposide in human lung adenocarcinoma cells. *Cancer Chemotherapy and Pharmacology*, *43*(1), 29–34. https://doi.org/10.1007/s002800050859

Ubrich, N., Bouillot, P., Pellerin, C., Hoffman, M., & Maincent, P. (2004). Preparation and characterization of propranolol hydrochloride nanoparticles: A comparative study. *Journal of Controlled Release*, *97*(2), 291–300. https://doi.org/10.1016/j.jconrel.2004.03.023

Valko, M., Rhodes, C. J., Moncol, J., Izakovic, M., & Mazur, M. (2006). Free radicals, metals and antioxidants in oxidative stress-induced cancer. *Chemico-Biological Interactions*, *160*(1), 1–40. https://doi.org/10.1016/j.cbi.2005.12.009

Vandervoort, J., & Ludwig, A. (2002). Biocompatible stabilizers in the preparation of PLGA nanoparticles: A factorial design study. *International Journal of Pharmaceutics*, *238*(1–2), 77–92. https://doi.org/10.1016/S0378-5173(02)00058-3

Vargas, A. J., & Burd, R. (2010). Hormesis and synergy: Pathways and mechanisms of quercetin in cancer prevention and management. *Nutrition Reviews*, *68*(7), 418–428. https://doi.org/10.1111/j.1753-4887.2010.00301.x

Vashisth, P., Singh, R. P., & Pruthi, V. (2015). A controlled release system for quercetin from biodegradable poly(lactide-co-glycolide)-polycaprolactone nanofibers and its in vitro antitumor activity. *Journal of Bioactive and Compatible Polymers*, *31*(3), 260–272. https://doi.org/10.1177/0883911515613098

Vijayababu, M. R., Kanagaraj, P., Arunkumar, A., Ilangovan, R., Aruldhas, M. M., & Arunakaran, J. (2005). Quercetin-induced growth inhibition and cell death in prostatic carcinoma cells (PC-3) are associated with increase in p21 and hypophosphorylated retinoblastoma proteins expression. *Journal of Cancer Research and Clinical Oncology*, *131*(11), 765–771. https://doi.org/10.1007/s00432-005-0005-4

Wang, W., Sun, C., Mao, L., Ma, P., Liu, F., Yang, J., & Gao, Y. (2016). The biological activities, chemical stability, metabolism and delivery systems of quercetin: A review. *Trends in Food Science and Technology*, *56*, 21–38. https://doi.org/10.1016/j.tifs.2016.07.004

Wang, X., Yu, D. G., Li, X. Y., Bligh, S. W. A., & Williams, G. R. (2015). Electrospun

medicated shellac nanofibers for colon-targeted drug delivery. *International Journal of Pharmaceutics*, *490*(1–2), 384–390. https://doi.org/10.1016/j.ijpharm.2015.05.077

Watson, D. G., & Oliveira, E. J. (1999). Solid-phase extraction and gas chromatography – mass spectrometry determination of kaempferol and quercetin in human urine after consumption of Ginkgo biloba tablets. *Journal of Chromatography B*, *723*, 203–210.

WHO. (2010). Background Paper: Non-communicable diseases in low- and middle-income, (October), 1–14. https://doi.org/25-26 October 2010

Wilson, B., Samanta, M. K., Santhi, K., Kumar, K. P. S., Paramakrishnan, N., & Suresh, B. (2008). Poly(n-butylcyanoacrylate) nanoparticles coated with polysorbate 80 for the targeted delivery of rivastigmine into the brain to treat Alzheimer's disease. *Brain Research*, *1200*, 159–168. https://doi.org/10.1016/j.brainres.2008.01.039

Wu, T.-H., Yen, F.-L., Lin, L.-T., Tsai, T.-R., Lin, C.-C., & Cham, T.-M. (2008). Preparation, physicochemical characterization, and antioxidant effects of quercetin nanoparticles. *International Journal of Pharmaceutics*, *346*(1–2), 160–168. https://doi.org/10.1016/j.ijpharm.2007.06.036

Young J. Moon, Liang Wang, R. D. and M. E. M. (2008). Quercetin Pharmacokinetics in Humans. *Biopharmaceutics & Drug Disposition*, *29*(4), 205–217. https://doi.org/10.1002/bdd

Yu. Shekunov, B., Baldyga, J., & York, P. (2001). Particle formation by mixing with supercritical antisolvent at high Reynolds numbers. *Chemical Engineering Science*, *56*(7), 2421–2433. https://doi.org/10.1016/S0009-2509(00)00443-7

Zhang, Z. B., Shen, Z. G., Wang, J. X., Zhao, H., Chen, J. F., & Yun, J. (2009). Nanonization of megestrol acetate by liquid precipitation. *Industrial and Engineering Chemistry Research*, *48*(18), 8493–8499. https://doi.org/10.1021/ie900944y

Zhao, H., Wang, J. X., Wang, Q. A., Chen, J. F., & Yun, J. (2007). Controlled liquid antisolvent precipitation of hydrophobic pharmaceutical nanoparticles in a MicroChannel reactor. *Industrial and Engineering Chemistry Research*, *46*(24), 8229–8235. https://doi.org/10.1021/ie070498e